DROP ON DEMAND TECHNOLOGY AS A MINI MANUFACTURING PLATFORM FOR DRUG DELIVERY AND PERSONALIZED MEDICINE

By

ABHISHEK SAHAY

A thesis submitted to the

Graduate School-New Brunswick

Rutgers, The State University of New Jersey

and

The Graduate School of Biomedical Sciences

University of Medicine and Dentistry of New Jersey

in partial fulfillment of the requirements

For the degree of

Master of Science

Graduate Program in Biomedical Engineering

Written under the direction of

Professor Paul Takhistov

And approved by

_____

_____

_____

New Brunswick, New Jersey

January 2012

ABSTRACT OF THE THESIS

Drop on Demand Technology as a mini manufacturing platform for Drug Delivery and Personalized Medicine

By ABHISHEK SAHAY

Thesis Director:
Dr. Paul Takhistov

There is need to develop a process and technology through which small tailored dosages can be delivered with precision and accuracy. This has led to research on developing a manufacturing platform which could be used to deliver personalized drugs in a variety of dosage formats both cheaply and efficiently. We envision a mini manufacturing platform centered on Drop-on-Demand (DoD) technology which can have wide ranging applications such as personalized medicine, clinical trials, poly-pharmacy and distributed manufacturing. A prototype system has been developed that has been tested for accuracy using gravimetric methods for dispensing sample dosage formats. The incorporation of online analytics has also been explored.

Three sets of experiments were conducted. In the first one, the accuracy of the system was measured experimentally using gravimetric methods. The dispensing system was found to be very accurate with RSD < 1% and this was true for dispensing solutions as well as suspensions. In the second experiment the effect of viscosity was studied. It was found that for a fixed set of variables such as input pressure and nozzle diameter there was a limiting viscosity above which the dispensing was disrupted. The aggregation

behavior of suspensions during flow through micro capillary was also studied. Finally the applicability of Raman spectroscopy for in line analytics was tested experimentally. It was found that Raman can be used for qualification of API in-capsule as well as in the supply line.

ACKNOWLEDGEMENT

I would like to profusely thank my advisor, Dr. Paul Takhistov who, during the last five years, has guided me with his profound academic knowledge and rich experience in numerous ways. From the selection of courses to the writing of my papers and dissertation, from experimental setup to discussion and analyses of the experimental results, Dr. Takhistov has guided me and put significant effort into my graduate study and research. I really admire his enthusiasm for scientific research and his kind patience with students.

I would also like to thank my parents, Praveen and Shashi Sahay, my uncle Dr. V.B. Mathur and my fiancé Shalini Jain. With their strong and continuous support, I have been able to successfully complete my studies.

Table of Contents

Abstract……ii

Acknowledgement……...……...iv

List of Figures……vi

Lists of Tables……viii

1. Introduction 1
   1.1. Drug Manufacturing Process 4
   1.2. Pharmaceutical Formulations 6
   1.3. Personalized Medicine/ Dosing Poly-pharmacy 9
   1.4. Quality assurance requirements in manufacturing (PAT) 12
   1.5. Mini Manufacturing Platform 15
   1.6. Critical liquid handling parameters 18
   1.7. Current Dispensing Techniques and Limitations 19
2. Drop Formation 20
   2.1. Ejection and stretching of liquid 21
   2.2. Necking and Pinch-off of Liquid Thread from Nozzle 21
3. Gravimetric Control 23
   3.1. Materials and Methods 23
   3.2. Results 23
   3.3. Discussion 24
4. Testing Viscosity Constraints 26
   4.1. Materials and Methods 26
   4.2. Results 28
5. Aggregation 30
   5.1. Material and Methods 43
   5.2. Results 44
6. In Line Analytics 46
   6.1. Materials and Methods 48
   6.2. Results 52
   6.3. Optimization of Raman probe position regarding the capsule 68
   6.4. Determination of the optimal exposure time 69
   6.5. Capsule filling process: analytical considerations 70
7. Discussion 73
   7.1. Unit dosage application: Filling mode 73
   7.2. Unit dosage application: Printing mode 74
8. Conclusion 78
9. List of References 82

Lists of Figures

Figure 1 Preparation of a pharmaceutical product 5
Figure 2 Classification of dosage forms according to physical properties 8
Figure 3 Dosing classification based on dispensing mode 10
Figure 4 Building blocks for PAT 12
Figure 5 Process design and analysis of critical process parameters 14
Figure 6 Design Strategy for Platform 16
Figure 8 Prototype Mini Manufacturing Platform 17
Figure 9 Sequence of images for Drop Formation generated using COMSOL 22
Figure 10 Schematic of Gravimetric system 23
Figure 11 Correlation between opening time of the valve and fluid mass dispensed after 100 cycles: ■ - chlorpropamide (H_2O: EtOH),▲- chlorpropamide (H_2O: EtOH: PEG), ▲- dopamine hydrochloride (H_2O: EtOH) and ◆- dopamine hydrochloride(H_2O: EtOH: PEG) 24
Figure 12 Viscosity Profile of Castor Oil Ethanol mixture 28
Figure 13 Weight of 100 drops as function of viscosity 29
Figure 14 Van der Walls interaction energy for different sized particles 33
Figure 15 Electrostatic Repulsive Energy for two latex particles of same size for different surface potentials and separation distances 36
Figure 16Poiseuille Flow in a Cylindrical Nozzle 38
Figure 17 Flow Profile 39
Figure 18 Variation of Reynolds Number as a function of Pressure for Poiseuille Flow (Red) and Lohms (black) 41
Figure 19 Effect of Shear Force on aggregation behavior: on top we see that during approach of particles drag force adds to the aggregation potential increasing the primary area of stability in the DLVO curve. On the bottom as the particles move away from each other shear acts in an opposite manner 43
Figure 20Particle Size distribution for .1% griseofulvin suspension in water before (blue) and after (red) dispensing through the system 44
Figure 21 .1% griseofulvinsuspension in three different solutions of HPMC (.1% .25% 1%) 45
Figure 23 Basic configurations of Raman spectroscopic set-ups with respect to the capsule sample. 50
Figure 22 Schematic for In Line Control 50
Figure 24 Schematics for backscattering mode in capillary 53
Figure 25 Effect of flow rate on Raman Spectra 54
Figure 26 Ibuprofen in ethanol was used to show the increase of intensity with increasing drug concentration for different wavelengths. 54
Figure 27 Schematics for Transmission mode 55
Figure 28 Spectral data for solution from transmission mode compared to standard spectra of pure materials (Ibuprofen and ethanol). The graph shows spectral changes with respect to exposure time 56
Figure 29 Schematics for back scattering mode for detection in capsule 57
Figure 30 Raman Spectra for Ibuprofen powder, ethanol and castor oil 59

Figure 31 Comparative Raman spectra crystalline drug in powder form, API solution, and un-filled capsule. 60
Figure 32 Shift of Raman spectra of ibuprofen in the region of the band at 1600 cm−1. 61
Figure 33 Raman spectra of hard gelatin capsule filled with Ibuprofen solutions at various concentrations 62
Figure 34 Resulting calibration with ordinary least square regression: measured Raman intensity from the API (△) and predicted values of the Raman signal (○) 65
Figure 35 Linearity shows validation of the Raman spectroscopy using UV spectroscopy for solutions. 66
Figure 36 Indomethacin suspension Raman spectroscopy calibration curve. 67
Figure 37 Determining of the optimal focusing distance foe the Raman measurement ... 68
Figure 38 Determining optimal exposure time 69
Figure 39 Simplified schematics of the capsule filling process with on-line Raman measurements 70
Figure 40 Estimated relative standard deviation of the measured API content as function of the scanning productivity 72
Figure 41 Filling vial with drug formulation via two-nozzle microdispensing set-up. Pharma-grade coloring agents have been added for visualization purposes 74
Figure 42High-speed imaging of the dopamine hydrochloride printing and resulting surfaced patterns produced through manipulation of key process parameters: (a) ramp of variable valve opening times, (b) regular square lattice array pattern, (c) printed array with overlapped API elements 76
Figure 43 Deposition of API's onto Tablets 77

Lists of Tables

Table 1 List of terms used..... 42
Table 2Ibuprofen associated Raman bands assignment obtained from DFT calculations and experimentally..... 58
Table 3 Parameter estimates and statistics for Ibuprofen data..... 64
Table 4 Droplet Diameter and Droplet Weight..... 77

1. Introduction

Commercially available medicines are generally available in only a few discrete doses. In cases where delivery of a precise dose is paramount, such as for highly potent actives, drugs with a narrow therapeutic index, or pediatric formulations (where the dose is based on body mass), the individual dosage unit may need to be divided prior to administration. Several studies have reported a lack of medication dose uniformity when breaking tablets into smaller units (van Santen, Barends et al. 2002). Another opportunity to deliver solid doses individually is to select a defined number or volume of drug-loaded particles (Wening and Breitkreutz 2011). This concept comprehends powders, granules, pellets or mini-tablets, but control of dose uniformity is still challenging during mini-tablet manufacture, and the exact dose cannot be varied in proportion to patient body mass. Perhaps the best methodology would be to have a manufacturing process that allows precise control, and extemporaneous preparation, of dose on a patient-to-patient basis. One of the most promising and forward thinking technologies that can be employed in the design of controlled release delivery and precise dosage formulations for small-scale manufacturing systems is Drop-on-Demand (DoD) technology.

Despite of all the research conducted, fundamental understanding of drop formation and impaction is still lacking(Hongming 2006). Considering the complexity of inkjet nozzle design and actuating mechanism, rheological and physiochemical properties of the inkjet inks, variety of the substrates, and interactions among them, making inkjet printing an industrial fabrication tool is challenging(Hongming 2006). The main research needs in

realization of this approach are to modify existing small scale micro-dosing equipment to include the drop-on-demand capabilities, and formulation materials need to be researched in order to create formulation platforms that can be used to generate small numbers of product units with precisely controlled *in vivo* performance. Important technology requirements for the system include:

- ability to predict the desired formulation for an active pharmaceutical ingredients (API) to achieve desired drop formation and solidification;
- ability to predict optimum conditions required to form drops with specific size required by dosage performance targets;
- accurate prediction of droplet impact, spreading phenomena, adhesion, and drug penetration;
- understanding and control of the final microstructure and stability of the splat;
- real-time process management capability.

The potential for use of technology in the pharmaceutical industry has only been explored in the last decade. There have been proof of concept studies in various applications such as delivery of poorly soluble drugs(Pardeike, Strohmeier et al.), printing API's onto edible films(Sandler, Määttänen et al. 2011), spray deposition of drugs (Rezvanpour and Wang 2011) etc. Dispensing has also been promoted as a delivery mechanism for personalized medicine. However there has been little discussion on how this technology could be incorporated into a future drug delivery platform.

One of the major problems that need to be addressed is to create a design space for developing a formulation based on dispensing system. Some technologies are suited for a range of variables and others for a different set. Another problem is the qualification of dispensed API. The industry is being pushed towards PAT for on/in/at line testing and a new manufacturing platform should be designed taking these factors into consideration. How and at which point can spectroscopic analysis is incorporated needs to be discussed and implemented.

In this thesis we are presenting a newly developed lab-scale modular system for microdosing application of pharmaceutically relevant compounds. In section 2 we look at the mechanics behind drop formation in an inkjet nozzle using modeling. In section 3we test the applicability of gravimetric control as part of an integrated measurement system. In section 4 and 5 we look at the look at the effects of rheological properties of the formulation such as viscosity and particle size on dispensing. Section 6 proposes incorporating Raman technology for inline monitoring of Active Pharmaceutical Ingredient (API) content as per PAT guidelines. We envision creation of a design space to predict system performance based on formulation properties. Finally, we demonstrate the application of the designed system for preparing different dosage formats for personalized medicine/dosing.

1.1. Drug Manufacturing Process

The drug manufacturing industry has produced a variety of medicinal and other health-related products undreamed of by even the most imaginative apothecaries of the past. These drugs have saved the lives of millions of people from various diseases, and they permit many ill people to lead reasonably normal lives.

Pharmaceutical manufacturing is divided into two major stages (Figure 1): the production of the active ingredient or drug (primary processing, or manufacture) and secondary processing, the conversion of the active drugs into products suitable for administration. The manufacture of pharmaceuticals is controlled by Good Management Practices (GMP) in some countries(Group 1998). Standard processes and guides to good manufacturing practice for medicinal products: play a central role in establishing criteria which guarantee the consistent production of safe and effective drugs. It is very difficult to gear current bulk manufacturing process towards small scale manufacturing. Major advantages of a platform include the fact that most steps downstream of the API synthesis can be eliminated. In fact, after the final purification and/or crystallization, the drug solution or suspension, including further printing additives, can be filled in cartridges. Alternatively, in case of limited drug stability in solution, a dry powder can be provided with an appropriate solvent in a two compartment container. These pre-packed drug containers are delivered to pharmacies or care providers, effectively eliminating most steps in association with powder processing, such as blending, milling, sieving, granulation, compaction and coating of solid forms.

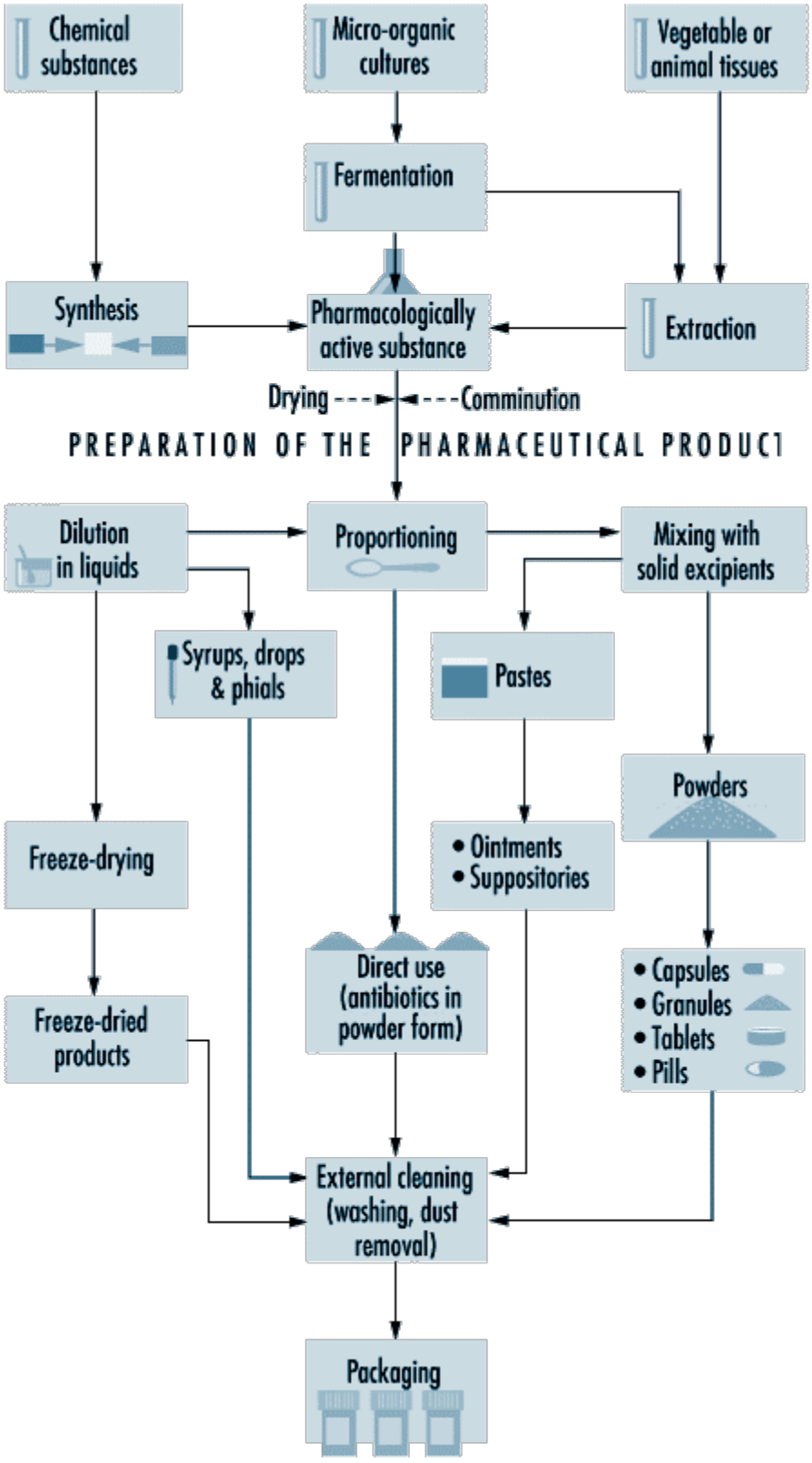

Figure 1 Preparation of a pharmaceutical product

1.2. Pharmaceutical Formulations

Pharmaceutics is the science of dosage form design. There are many chemicals with known pharmacological properties but a raw chemical is of no use to a patient. Pharmaceutics deals with the formulation of a pure drug substance into a dosage form. Active pharmaceutical ingredient (API) is a chemical compound with pharmacological (or other direct effect) intended for use in diagnosis, treatment or prophylaxis of diseases.

Direct administration of active drug substances is rare for a number of reasons. Firstly, API handling and accurate dosing can be difficult or impossible for low mg and mg doses. Also, API administration can be impractical, unfeasible or not according to the therapeutic aims. Some API can benefit from reducing the exposure to the environmental factors (light, moisture etc.), or they need to be chemically stabilized due to their inherent chemical instability. API can be degraded at the site of administration and can cause local irritations or injury when they are present at high concentrations at the site of administration (e.g., low pH in stomach).API can have unpleasant qualities such as bad taste or smell which can lead to reduced patient compliance. Finally, administration of active substance would mean to have no chance for modification (improvement) of its pharmacokinetic profile.

In order to go from drug substance to pharmaceutical preparation, besides the choice of the active drug substance, one needs to also make a responsible decision regarding the route of administration and the Dosage Form (drug delivery system) – the wrong choice of delivery system can cause failure of therapy.

Pharmaceutical dosage form determines the physical form of the final pharmaceutical preparation. Dosage forms can be classified as under according to their physical properties(Figure 2) ((Ancel 2011)).

- Gaseous Dosage Forms

Medicinal gases, inhalation/volatile anesthetics (vaporized before administration by inhalation), Aero dispersions of solid particles (e.g., anti-asthmatic inhalations) or liquid particles (anti-asthmatic inhalations or sprays)

- Liquid Dosage Forms

These can be in the form of solutions which have one homogenous phase, prepared by dissolving one or more API's in a solvent. Emulsion is dispersion system consisting of two immiscible liquids and can be either oil in water (o/w) or water in oil (w/o). Emulsions in general have a cloudy appearance. Suspensions are a dispersion system where solid particles (dispersed phase) are dispersed in liquid phase (dispersion medium). The dispersed particles range in size from nano to micro emulsions which vary their rheological properties.

- Semi-Solid Dosage Forms

There are a number of semi-solid dosage forms. Gels are semisolid systems in which a liquid phase is constrained within a 3D cross-linked matrix. Creams are semi-solid emulsion systems (o/w, w/o) containing more than 10% of water. Ointments are dosage forms which have (hydrocarbon ex. vaseline), water-soluble (PEG) or emulsifying base. Pastes are semisolid dispersion system, where solid particles (> 25%, e.g. ZnO) are dispersed in ointments – mostly oleaginous (Petrolatum).

- Solid Dosage Forms

These can be either in the form of bulk powder which is for external/internal use or shaped in the form of tablets and capsules etc.

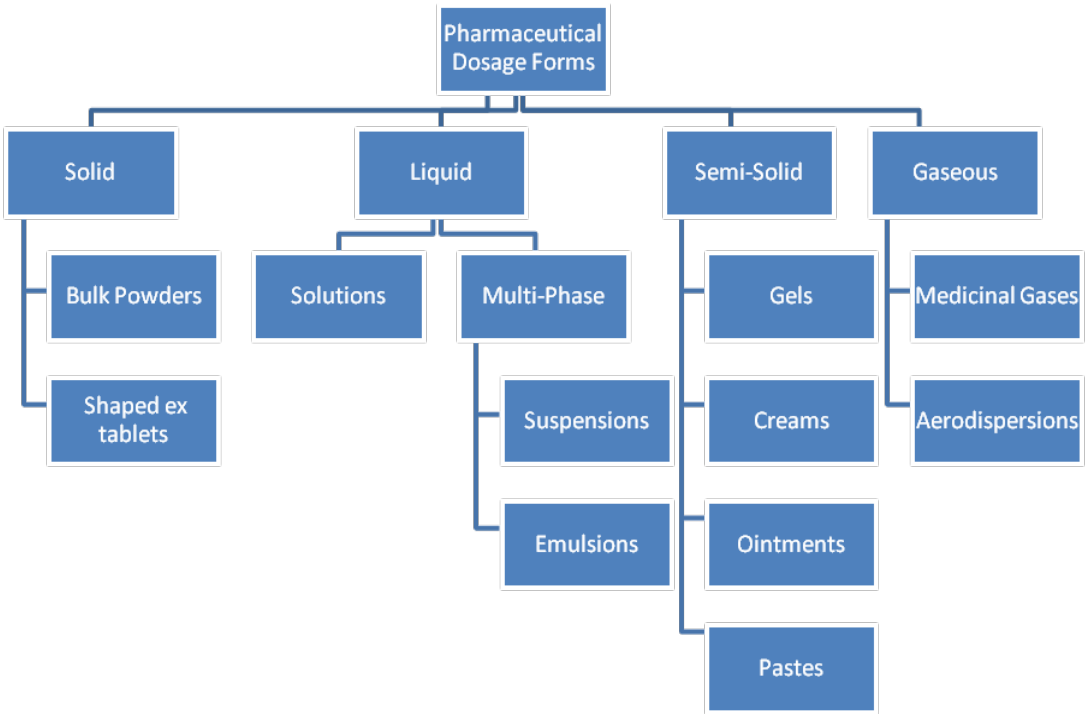

Figure 2 Classification of dosage forms according to physical properties

1.3. Personalized Medicine/ Dosing Poly-pharmacy

With the advent of the discoveries made in the human genome project genetic and anthropometric information about individuals can be utilized to deliver tailored strategies for the detection, treatment, and prevention of disease. Individuals react to and metabolize medications differently, and therefore require different doses of medications. Two approaches can be utilized to determine dosage:

(1) Pharmacogenomics (genetic information) and

(2) Environmental Factors (body mass, age, etc.).

For this "Personalized Medicine", only a few dosage options are available and the successful "translation" of these therapies to clinical application is totally dependent on the drug /formulation delivery platform.

Microdispensing and, in particular, Drop on Demand technology is an optimum technology to employ in this avenue because it allows for the delivery of customizable drug architecture due to its innovative and modular design. enables customization for use in personalized medicine because it is based upon a building block methodology where dosage and the drug delivery system is adapted by determining key attributes and combining the Active Pharmaceutical Ingredient (API) and polymer in a block matrix system.

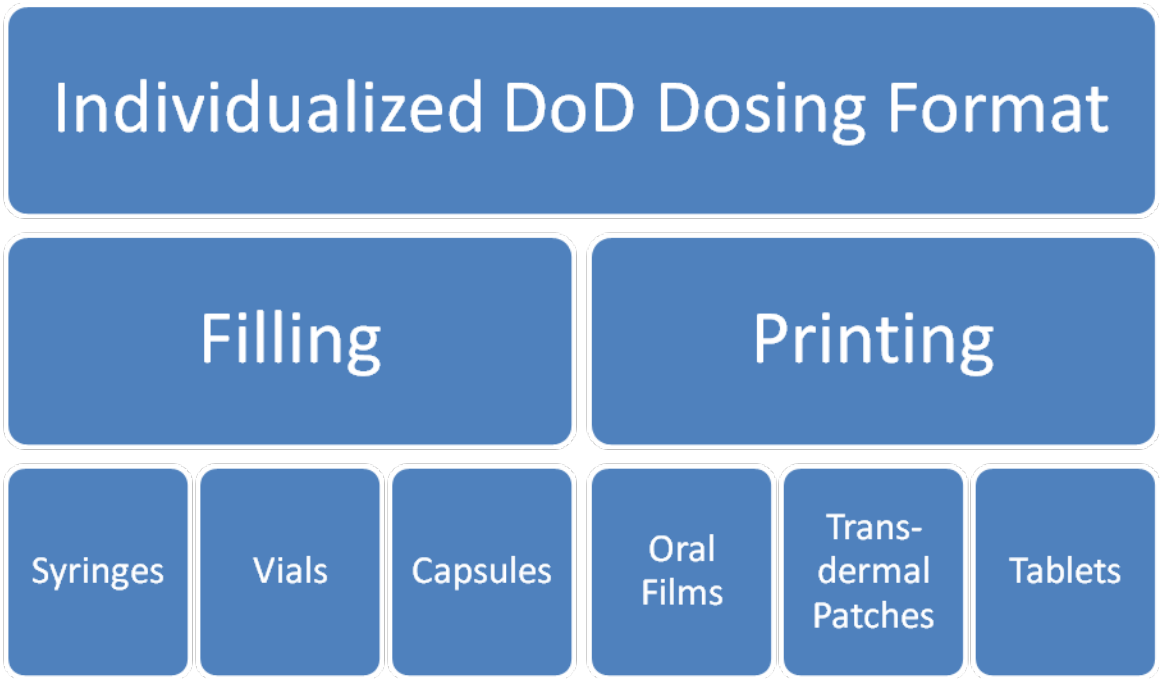

Figure 3 Dosing classification based on dispensing mode

Personalized medicine summarizes concepts and methods that aim to achieve an individualized therapy specifically tailored to the requirements and needs of an individual patient. Conventional dosage forms, such as tablets or capsules, provide predefined contents of the APIs. As a consequence, many patients, particularly women, children and elderly persons, may be confronted with under- or overdosage, which can lead to reduced or counter-productive effects. In personalized medicine, factors such as age, weight, height, race and gender-related aspects of the individual patients can be considered and translated in precisely tailored oral delivery forms.

For example, in pediatric healthcare, medications with the appropriate dosage are often not commercially available and only exist for a minority of drugs. To overcome this, the common practice is to cut tablets originally produced for adults into smaller portions to acquire lower dosages for children. However, this is imprecise because tablets cannot be

split accurately. Another practice to prepare drugs for children is the conversion of a commercially available solid medication (tablet or capsule) into a liquid dosage form by dissolution of the solid in a solvent. This procedure is challenging and creates a lot of uncertainties — interactions with excipients, increased toxicity, decreased efficacy or instability of the medication are just some of the shortcomings of this practice.

Gender studies have found that there can also be quite large differences between male and female patients in both drug efficacy and adverse drug reaction (ADR) because of differences in body weight, body composition, metabolizing enzymes or hormone concentrations. These factors can influence the pharmacokinetics and pharmacodynamics of medications, such as antidepressants or other drugs. An adjustment of the dosage on a daily basis depending on the sex of the patient is, therefore, crucial. Also the consideration of female test persons in clinical studies is important for the development of personalized drugs; an FDA regulation from 1998 demands equal male and female representation in clinical trials to change dosing guidelines.(Johannes G. Khinast 2011)

There are an increasing number of chronically sick people who take a significant number of different medicines each day. Fine tuning of these regimes in collaboration with the various health professionals in response to efficacy of treatment and management of side effects means these doses change often. The increasing age profile of the population means this situation is unlikely to diminish, and so new and innovative methods of drug therapy are required. Furthermore, the possibility of routine genomic screening of patients and the consequent need for personalized medicines present a significant challenge to current bulk manufacturing methods of standardized dosage forms.

1.4. Quality assurance requirements in manufacturing (PAT)

Historically, pharmaceutical production involves the manufacture of the finished product, followed by laboratory analysis to verify quality. The disadvantages associated with this approach are continual process optimization, recurring manufacturing difficulties, and the possibility of failed batches.

Process analytical technology (PAT) has been defined by the United States Food and Drug Administration (FDA) as a mechanism to design, analyze, and control pharmaceutical manufacturing processes through the measurement of Critical Process Parameters (CPP) which affect Critical Quality Attributes (CQA)((FDA) 2004).

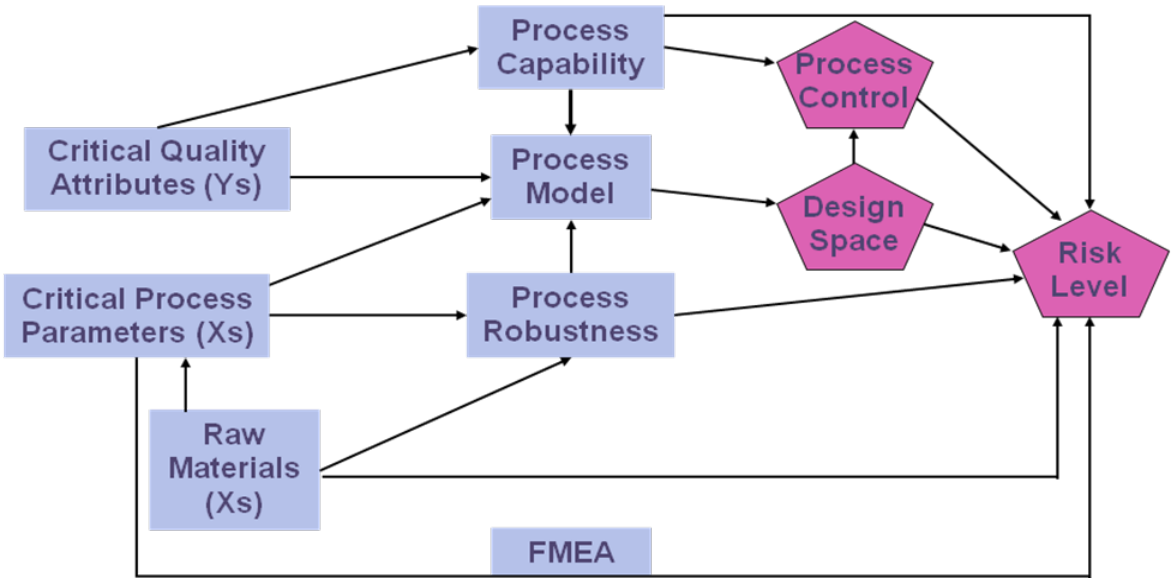

Figure 4 Building blocks for PAT

Process Analytical Technologies involve the use of raw material properties, manufacturing parameters, process monitoring, and chemometric techniques to produce

finished products of acceptable quality. The central point of PAT is to generate product quality information in real-time. The advantages of PAT are many and varied.

Raman is one of the techniques that have gained recent recognition as a means to add on or in-line analysis at the production level. Raman light source does not destroy or react with samples and is able to penetrate into and through solid samples. While Raman has gotten most of the attention, PAT is not limited to Raman but can include many other forms of monitoring, such as NIR, Mid-IR, acoustic emission signals, and other imaging techniques ((FDA) 2004; Gnoth, Jenzsch et al. 2007; Huiquan, Edwin et al. 2008).

As can be seen in the above discussion, the use of PAT techniques can lead to huge benefits. Process Analytical Technology provides better knowledge of raw materials, manufacturing parameters and their impact on finished product quality. PAT also lead to a more robust process, better products, more uniform dissolution results, and a huge cost savings for the manufacturer. The challenge that dissolution scientists face is to become familiar with this next generation of pharmaceutical testing and its potential applications. Utilizing the Food and Drug Administration (FDA) Process Analytical Technology (PAT) Guidelines we engineered a modular design which enables to gain process understanding through the measurement and analysis of critical process parameters. In addition, the integration of these technologies enables in-line monitoring and control and continuous real time quality assurance. Additional feedback control mechanisms include real time image control.

The process is monitored and controlled through a feedback mechanism in which the end-user can control process variables such as volumetric flow rate, dispensing time, acquisition time, and applied pressure. To ensure process accuracy critical process parameters are measured in-line utilizing gravimetric volume analysis, optical spectral analysis, and image acquisition.

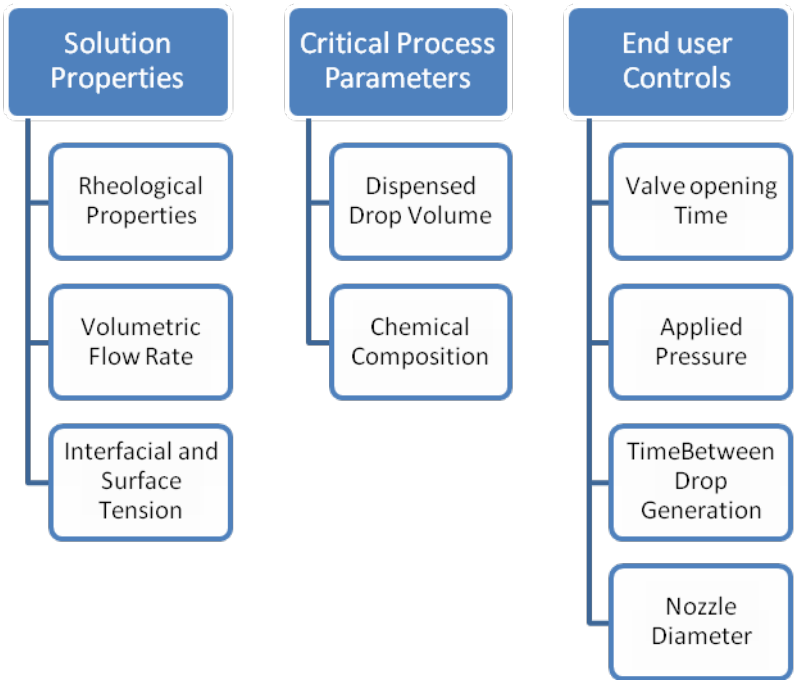

Figure 5 Process design and analysis of critical process parameters

1.5. Mini Manufacturing Platform

An approach based upon ink-jet printing of formulations to manufacture dosage forms which can be optimized to each patient in terms of dosage, release profiles and combination of drugs could address this challenge. In addition, the ubiquitous and inherently scalable nature of such technology would make implementation at the point of care and scaling of manufacture a possibility.

Based on the range of formulations we need a flexible and user friendly platform which can dispense a wide range of functional materials with a range of dispensing nozzles. It should modular in design with a room for scalability (Li, Saedan et al. 2009)have developed a multi nozzle system.

A manufacturing platform for delivery of pharmaceutical formulations needs to meet the flowing requirements:

Accuracy: Since the main objective of the system is dosing of API's it needs to be very accurate (RSD <3%). As the drugs are highly potent a slight variation in dosage can be toxic to the patient

Robustness: The system should not be perturbed by small variations in operational and environmental variables

Cost Since the objective of the platform is to be available for small batch manufacturing such as in clinical supply or pharmacy it needs to be a cost effective solution since a large number of units might be deployed.

Printing technology is cheap, yet affords extremely fine control of droplets, and hence uniformity of drug dose.

Software: The system needs to be completely automated at require minimum user input. Also due quality assurance requirements a large amount of data is generated and should be capable of handling it.

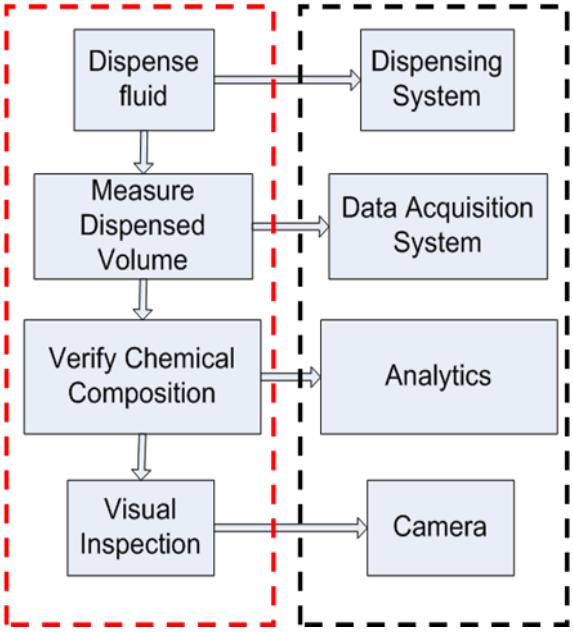

Figure 6 Design Strategy for Platform

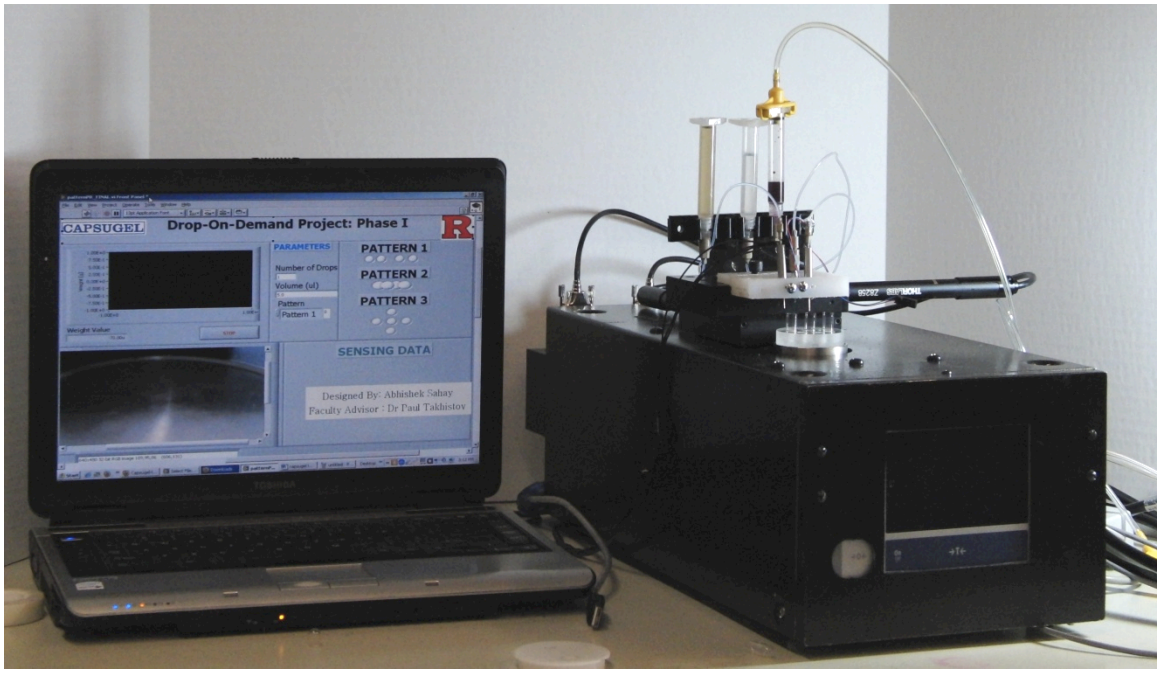

Figure 7 Prototype Mini Manufacturing Platform

1.6. Critical liquid handling parameters

Accuracy – This is a measure of how close an electromechanical system can approach a given goal, be it position in three dimensions or volume dispensed. Both are important for automated liquid handlers, providing limits for how small is the smallest volume that can be sampled

CV – Coefficient of Variation is essentially the standard deviation normalized to a percentage by dividing by the mean. This is usually how the precision of automated liquid handling system pipetting capabilities are given, as in 1 microliter ± 5%

Speed: it is a measure of how fast the dispensing system can actually dispense fluids, usually measured in drop per second.

Precision/repeatability – it is usually defined as the measure of how likely it is for an electromechanical system to achieve its goal.

Viscosity – it refers to the resistance of a fluid to shear motion, its internal friction. Water is a low viscosity fluid. Viscosities much higher than water can be a real challenge for automated liquid handling systems, as they have higher surface adhesion and lower surface wettability. High viscosity fluids will cause turbulent flow at lower flow rates than low viscosity fluids.

1.7. Current Dispensing Techniques and Limitations

In drug discovery, most automated liquid handling is accomplished using either syringe pump-based (i.e. displacement type) pipettors for transferring fluid that use a syringe coupled to a metal or plastic tip. Displacement by the syringe in turn displaces fluid from the tip. Typically, these devices can dispense over the range of microliters to milliliters. As an interim solution to provide dispensing, syringe pump pipettors can be configured to produce a small drop on the tip that can be touched to a dry surface for dispensing (touch-off dispensing). In the last decade various micro fluidic systems have been developed which attack the problem of dispensing nanoliter or even picoliter-quantities of different kinds of fluids. Some of them are quite similar to ink-jet print heads and use drop-on-demand technology for ejecting single liquid droplets in the range of some hundreds of nanoliters.

The use of inkjet dispensing technology generally provides several advantages over syringe-pump based liquid handling. As a non-contact printing process, the volumetric accuracy of ink-jet dispensing is not affected by how the fluid wets a substrate, as is the case when positive displacement or pin transfer systems “touch off” the fluid onto the substrate during the dispensing event. In addition, the fluid source cannot be contaminated by the substrate, as is the potential during pin transfer touching. In addition, because the technique is non-contact, delivery of the drop to a small location is not limited by the mechanical size of the tip. The ability to free fly the droplets of fluid over a millimeter of more allows fluids to be dispensed into wells or other substrate features (e.g., features that are created to control wetting and spreading).Finally, the speed of inkjet printing translates into high-speed dispensing when using these technologies.

2. Drop Formation

Three common methods of producing drops from an orifice are dripping, continuous jetting, and drop on demand jetting. Dripping occurs under the action of gravitational force when liquid exits a capillary tube at a low flow rate. Drop production rate is low as it takes a relatively long time (seconds to minutes) to generate one drop. Therefore, it is mainly employed in experimental devices including surface tension meters and contact angle analysis equipment. When the flow rate through the capillary tube is increased, transition from dripping to continuous jetting occurs. The continuous jet breaks into drops due to the Rayleigh instability. By introducing a cyclic disturbance, a stream of uniform drops can be produced with high speed and frequency. Continuous jetting has been successfully applied in inkjet printing, but requires a complicated control system. A drop generator ejects a small volume of liquid by applying a short pressure pulse to the liquid filling the channel. Under the right conditions, the volume of liquid exiting the nozzle evolves into a single drop. It is an efficient approach to deposit micron-scale drops on a substrate because it is easily controlled by tuning the driving electrical signal and is compatible with various materials. The dripping and continuous jetting processes have been investigated for approximately one century. Thorough re-views of related literature can be found in Eggers (Eggers 1997)Lin and Reitz(Lin and Reitz 1998), Furbank(Furbank and Morris 2004), and Subramani (Subramani, Yeoh et al. 2006)

2.1. Ejection and stretching of liquid

When the contracted transducer expands, liquid in the nozzle is accelerated and pushed out of the nozzle orifice. Initially, the meniscus then quickly extends outward until a liquid column with a round leading edge is formed (Figure 8-a). After a short time (starting at approximately (Figure 8-b), the liquid flow rate from the nozzle decreases. The difference in axial velocity between the column head and the liquid at the nozzle exit causes the liquid column to stretch. The speed of the liquid at the nozzle exit continues to fall until no additional liquid flows into the column and possibly even some liquid is sucked back into the nozzle due to the negative pressure associated with the second pulse of the waveform causing contraction of the piezoelectric transducer. The volume of the liquid column remains constant, and the inertia of the liquid continues to extend the column. The rate of extension decreases as new surface is created with the corresponding increase in the surface energy.

2.2. Necking and Pinch-off of Liquid Thread from Nozzle

During the stretching of the liquid column, the liquid at the tail (at the nozzle exit) necks. This necking position re-mains at the nozzle exit, and the radius of the liquid thread here continuously thins (Figure 8-c) .Thus, a long transitional liquid column is created, reaching from the nozzle to the head. Finally, the tail of the liquid thread pinches off from the nozzle exit, creating a free liquid thread with a bulbous head (Figure 8-d).

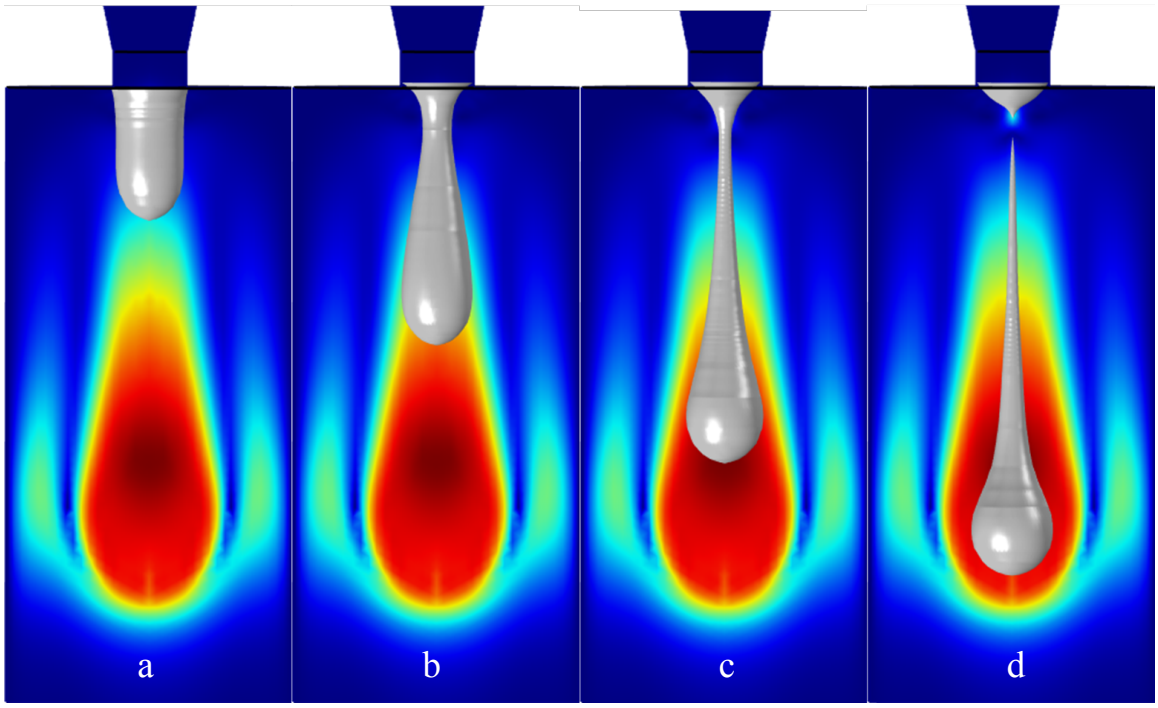

Figure 8 Sequence of images for Drop Formation generated using COMSOL

3. Gravimetric Control

3.1. Materials and Methods

The gravimetric system consisting of a weighting module (Figure 9), WM (WXSS205DU, Mettler Toledo, OH) interfaced with PC for automated weight recording, was placed on top of a motorized stage (OptiScan ES 103) which could be moved in the X & Y directions. The stage was operated through a LabVIEW interface. An in-line camera was also automatically controlled through LabVIEW. The weighting module and dispensing system was placed inside an acrylic box to prevent air current from altering the process performance; all electronics were mounted outside.

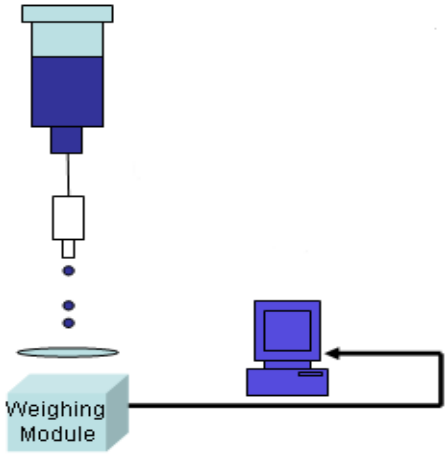

Figure 9 Schematic of Gravimetric system

3.2. Results

The linear correlation between the opening time for the valve and the mass of solution dispensed after 100 cycles is depicted in Figure 10. Different amounts of the different fluids pass through the valve while it is open for a specific period of time. The mass of liquid dispensed increases from Chlorpropamide/PEG to an H_2O/ethanol one. A

correlation can be seen between the viscosity and the mass of fluid dispensed. The correlation between valve opening time and mass dispensed in 100 cycles for all fluids is near perfectly linear with R^2=1, which is in good agreement with the theory (Lin and Reitz 1998).

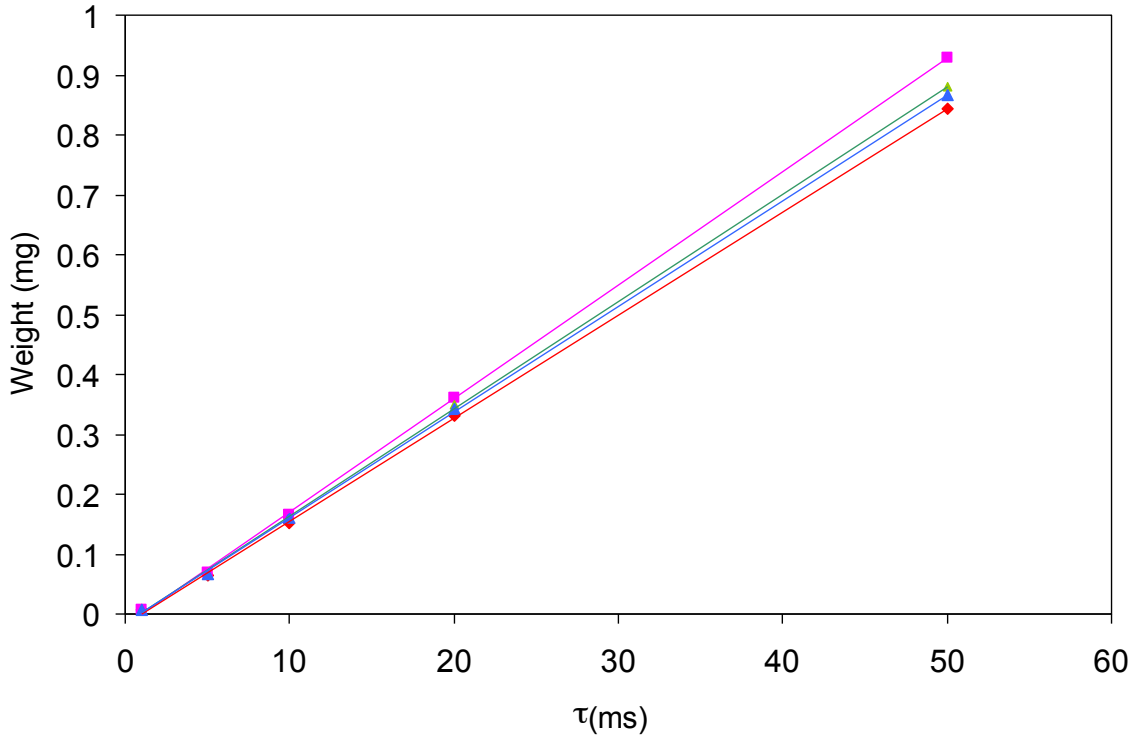

Figure 10 Correlation between opening time of the valve and fluid mass dispensed after 100 cycles: ■ - chlorpropamide (H_2O: EtOH), ▲ - chlorpropamide (H_2O: EtOH: PEG), ▲ - dopamine hydrochloride (H_2O: EtOH) and ◆ - dopamine hydrochloride(H_2O: EtOH: PEG)

3.3. Discussion

To characterize the droplet volume change under the feedback control, the dynamic response of weighting module was recorded. The real-time feedback control should converge as fast as possible to maintain a stable volume. Droplet volume can be regulated

via several process parameters: supplied gas pressure, nozzle diameter, and time of valve opening. A quite sophisticated feedback controller can be designed with the time of valve opening as control output and measurement mass of deposited droplet as control target. Since proportional control alone is not enough, integral and differential components may be added into the feedback control algorithm.

This improves the overall accuracy of operations. The discrete time proportional-integral-derivative (PID) feedback controller for the droplet volume control is:

$$\tau_{n+1} = K_i \tau_n + K_p \varepsilon_n + K_d \left(\varepsilon_n - \varepsilon_{n-1} \right) \qquad (1)$$

Where, τ_n is the time of valve opening for *n*-th droplet, ε_n is the error $\varepsilon_n = m_n - m_0$ with m_n, m_0- mass of generated *n*-th droplet and target droplet mass respectively. K_p And K_d are proportional and differential coefficients, respectively.

4. Testing Viscosity Constraints

Viscosity is the major variable that guides selection of dispensing system. The solenoid system has difficulty dispensing liquids with high viscosities. If the viscosity is very high (~ 80 cP) the droplet will not "jet" from the dispense tip. Fluid will begin to collect at the tip and dispense volumes will be very erratic. For example, there may be several dispenses where no drops leave the tip and then, after enough drops accumulate on the tip, there will be a large volume dispensed. If the viscosity is too high (> 100 cP), the fluid will not dispense at all. This limitation can be overcome up to an extent by increasing the air pressure, but this also has an upper limit.

4.1. Materials and Methods

Experiments were conducted to test the viscosity limits of the system. Castor oil (~ 800 cP) was chosen as a fluid with high density and carbitol cellosolve (~ 5 cP) and ethanol as the low viscosity fluids.

It was noticed that there was no flow out of the valve for pure castor oil. In order to decrease the viscosity it was heated up to 80 deg centigrade but the problem persisted. The applied pressure was also increased up to 60 psi, which is near the operable limit of the system but the oil was not dispensed. In order to determine the maximum viscosity at which the valve will be able to operate, a mixture of castor oil in ethanol was prepared with increasing amounts of castor oil from 0 to 100 %. The viscosity of the blend of two

or more liquids can be estimated using the Refutas equation. The calculation is carried out in three steps:

First the viscosity blending number (VBN) is calculated for each component in the mixture using the following equation:

$$VBN = 14.534 \times \ln\left[\ln\left(v + 0.8\right)\right] + 10.975$$

Where v is the kinematic viscosity in centistokes (cst). The kinematic viscosities must all be obtained at the same temperature. The VBN of the mixture is then calculated by weighting the component VBN's by mass fraction:

$$VBN_{BLEND} = \left[x_A \times VBN_A\right] + \left[x_B \times VBN_B\right]$$

Where x is the mass fraction of each component of the blend. The kinematic viscosity of the mixture can then be calculated using the inverse of the first equation:

$$v = \exp\left(\exp\left(\frac{VBN_{BLEND} - 10.975}{14.534}\right)\right) - 0.8$$

Where VBN_{Blend} is the viscosity blending number of the blend.

4.2. Results

Figure 11 shows the calculated values for the castor oil and ethanol mixture.

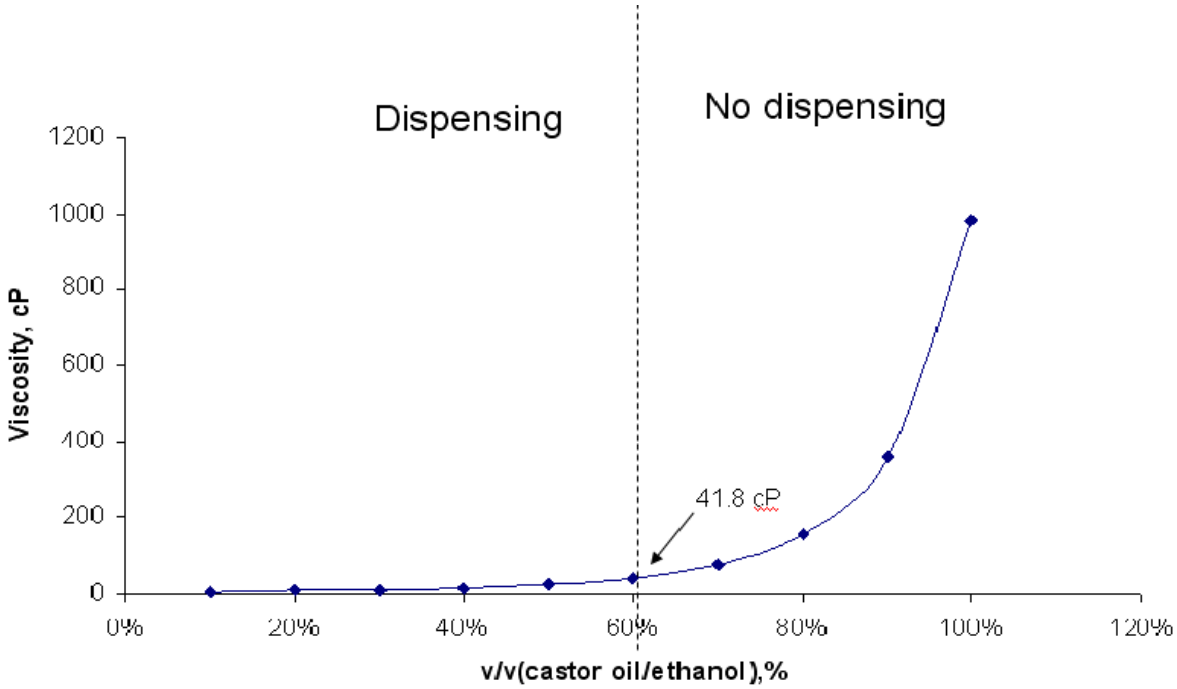

Figure 11 Viscosity Profile of Castor Oil Ethanol mixture

The viscosity increases in an exponential manner. By using mixtures with increasing concentration of ethanol with the valve, the approximate upper limit of jettable viscosity was determined. Figure 12shows the weight data for some of those mixtures. It can be seen that viscosity does not affect the accuracy of the drop volume as $R^2 > .99$.

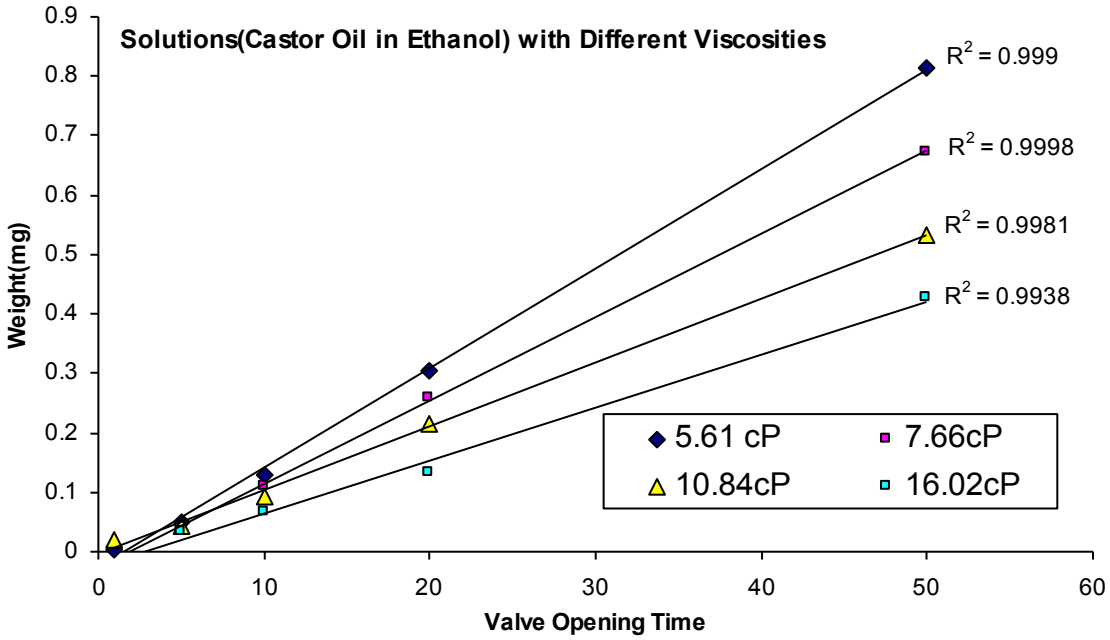

Figure 12 Weight of 100 drops as function of viscosity

5. Aggregation

In this section we investigate the mechanism of flocculation of a colloidal dispersion in an inkjet nozzle. Effect of parameters such as particle size, zeta potential and shear rate will be studied. By building a stability map for suspensions, guidelines for dispensable formulations can be prepared.

A number of liquid drug formulations are in the form of suspensions due to the solubility limits of various drugs. These fluids are complex with large variations in rheological properties due to factors like viscosity, particle size, surface tension etc. Such complex fluids can lead to a number of issues such as clogging of the nozzle, aggregation of drug particles etc. when subjected to the forces present inside the micro fluidic channel.

Pharmaceutical suspensions are thermodynamically unstable systems and subjecting them to forces present in a micro-dosing system can lead to their destabilization. The suspended drug particles interact in presence of the hydrodynamic and inter-particle force and it can lead to agglomeration. One method of understanding this phenomenon is to study orthokinetic aggregation. The process of aggregation of colloidal particles is a two part process. First, the particles must be brought close together. This could be due to different transport mechanisms such Brownian (perikinetic) motion or due to hydrodynamic forces. Once the particles approach each other inter-particle forces take over. If the net force is attractive aggregates will form, otherwise the particles will move away.

Inter-particle Forces

One of the basic problems in colloidal science is to find the net force acting between two or more particles. If the net force is attractive, particles will come together and for agglomerates leading to instability of the suspension. If the net force is repulsive the particles remain segregated and formulation remains stable. The inter-particle forces considered in this study are the attractive Van der Waals force and electrostatic repulsion force. The total interaction energy between two interacting particles is the sum of these forces and can be expressed as:

$$F_T=F_{DISP}+F_E \tag{1.2}$$

Where,F_T is the total interaction force, $F_{disp}$is the attractive Van der Walls force and, $F_E$is the repulsive electrostatic force.

Van Der Walls Interaction

Van der Wall's dispersion forces are forces acting between neutral atoms or molecules. There are three different types of forces, depending on the nature of the molecules. They are:

1) The attraction between permanents dipoles is called Keesom attraction and is given by:

$$V_{att} = -\frac{\mu^4}{(4\pi\varepsilon)^2 \kappa T R^6} \tag{1.3}$$

Where u is the dipole moment, ε the permittivity of the medium, kT the thermal energy, and R the distance between the molecules.

Debye or Induction interaction which results from the attraction of permanent and induced dipoles given by:

$$V_{att} = -\frac{\alpha\mu^2}{(4\pi\varepsilon)^2 R^6} \qquad (1.4)$$

Where α is the polarizability of the nonpolar molecule.

London Dispersion energy between dipoles of non-polar molecules or atoms given by:

$$V_{att} = -\frac{3\alpha^2 h\nu_0}{64\pi^2\varepsilon^2 R^6} \qquad (1.5)$$

Where $\frac{1}{2}h\nu_0$ is the ground state energy of the atom or molecule, h is the Planck's constant, and ν_0 is the frequency of the vibration.

All three types of dispersion forces or their combinations can be written as

$$V_{disp} = -\frac{\lambda}{R^6} \qquad (1.6)$$

For two colloidal particles, the dispersion energy can be calculated by adding the contribution of all the possible pair of atoms. This can be done by adding the contributions of all the possible pair of atoms called the Hamaker Summation Procedure. This gives us

$$V_{disp} = -\lambda n^2 \iint_{V_1 V_2} \frac{dV_1 dV_2}{r^6} \qquad (1.7)$$

Where n is the number of molecules per unit volume. For two unequal spheres with radius a_1 and a_2:

$$V_{disp} = -\frac{A(h)}{6}\left[\frac{2a_1a_2}{R^2-(a_1+a_2)^2}+\frac{2a_1a_2}{R^2-(a_1-a_2)^2}+\ln\frac{R^2-(a_1+a_2)^2}{R^2-(a_1-a_2)^2}\right] \quad (1.8)$$

Where h is the gap between spheres, $R-a_1-a_2$ and $A(h)$ is the Hamaker Constant. Typically, is of the order of 10^{-19}-10^{-21}J. Figure 13 shows the Van der wall interaction energy between particles of dissimilar radii based on equation(1.8). The x-axis shows the radius on one particle while the other is held constant at 100nm and the y-axis shows the particle separation. As the size difference increases, the interaction energy tends to saturate.

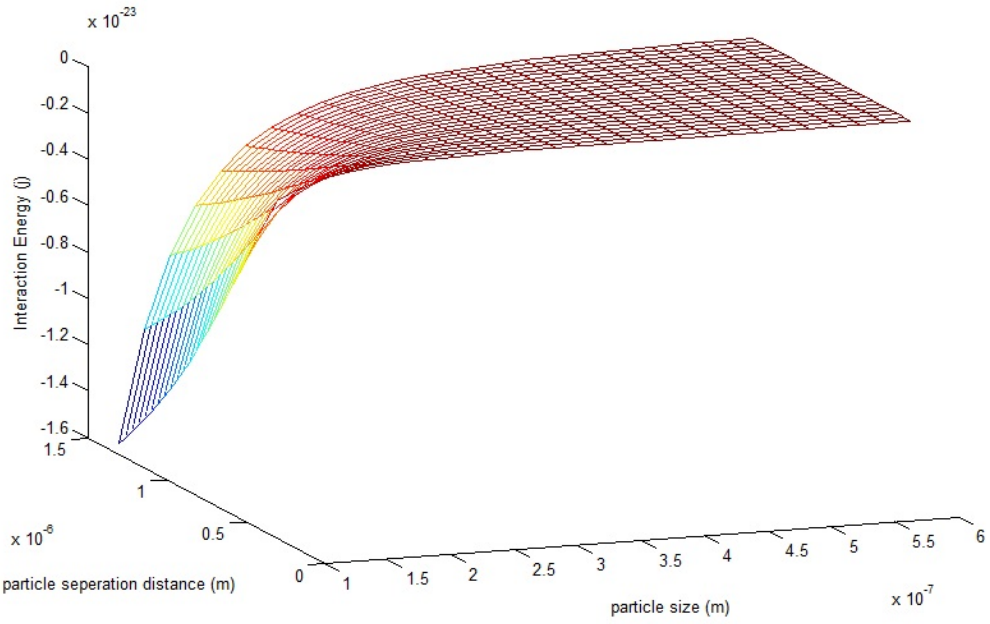

Figure 13 Van der Walls interaction energy for different sized particles

In equation (1.8) it is assumed that the electromagnetic interactions between atoms and molecules act instantaneously. In reality it takes certain time for an electromagnetic signal to travel back and for between two molecules. Because of this effect, the dispersion force is weakened or retarded when the molecules are far apart. The assumption of complete additivity is also a drawback and resulting expressions overestimate the interaction. Vanni found that by calculating Hamaker constant based on Lifshitz theory of dispersion which is capable of considering ionic screening we can create a fully predictive estimation of collision efficiency(Vanni and Baldi 2002):

$$A(h) = A_{\varepsilon=0} * (1+2kh)e^{-2kh} + A_{(\varepsilon>0)} * f(h) \tag{1.9}$$

Where $A_{(\epsilon=0)}$ and$A_{(\epsilon\to 0)}$ are two constant, whose value depends on the considered systems and that summarize the effect of zero and non zero frequency components respectively. $f(h)$is the function for retardation effect that decays from 1(at h=0) to 0($h \to \infty$). K is the inverse Debye length, $k = F\sqrt{2I/(\varepsilon_r \varepsilon_o RT)}$, which depends on the ionic strength of the solution, *I*.

By expanding analytically the derivative of the interaction

(1.10)

$$F_{disp} = \frac{dV_{disp}(h)}{dh} = -\frac{1}{6}\left[4k^2 he^{-2kh}A_{(\varepsilon=0)} - \frac{\left[f(h)\right]^{5/2}}{h}(\left[f(h)\right]^{-3/2} - 1]A_{(\varepsilon=0)}\right] *$$
$$\left[\frac{2a_1a_2}{R^2-(a_1+a_2)^2} + \frac{2a_1a_2}{R^2-(a_1-a_2)^2} + \ln\frac{R^2-(a_1+a_2)^2}{R^2-(a_1-a_2)^2}\right]$$
$$-\frac{32}{3}\left[A_{(\varepsilon=0)}(1+2kh)e^{-2kh} + A_{(\varepsilon>0)}f(h)\right]\frac{Ra_1{}^3a_2{}^3}{\left[R^2-(a_1+a_2)^2\right]^2\left[R^2-(a_1-a_2)^2\right]^2}$$

This expression has been used to calculate the Van der Walls force.

Electrostatic Repulsion Interaction Energy

In most cases colloidal particles possess an electronic charge and because the dispersion as a whole must be electrically neutral, it follows that there must be an excess of ions of opposite charge in solution. These charges occur in the neighborhood of the suspended colloidal particles giving rise to a diffuse (electrical) double layer. When two colloidal particles-each surrounded by an electrical diffuse double layer-approach each other, their double layers begun to overlap which results in an increase in energy for the two particles. The resultant force can be calculated using the classical expression by Hogg Healy(Hogg, Healy et al. 1966):

$$F_E = 4\pi\varepsilon_0\varepsilon_{r,m}\psi_p{}^2 \frac{a_1 a_2}{a_1 + a_2} \frac{k(1-e^{-kh})}{e^{kh} - e^{-kh}} \tag{1.11}$$

Where φ_p is the surface potential, ε_0 is the free space permittivity and $\varepsilon_{r,m}$ is the static dielectric permittivity of the medium. According to Sader (Sader, Carnie et al. 1995) this expression is accurate for large ka and small kh so they modified this formula to work over a greater range of values. For a couple of particles of the same material interacting at low constant surface potential the expression by Sadder is:

$$F_E = 4\pi\varepsilon_0\varepsilon_{r,m}\psi_p{}^2 \frac{a_1 a_2}{a_1 + a_2} \left[\frac{\ln(1+e^{-kh})}{a_1 + a_2 + h} + \frac{k(1-e^{-kh})}{e^{kh} - e^{-kh}} \right] \tag{1.12}$$

While at high potential (ψ_p>25mv) it is:

$$F_E = \frac{64\pi\varepsilon_0\varepsilon_{r,m}\psi_p{}^2 a_1 a_2}{a_1 + a_2 + h} \left[\frac{\ln(1+e^{-kh})}{a_1 + a_2 + h} + \frac{k(1-e^{-kh})}{e^{kh} - e^{-kh}} \right] \left[\frac{K_B T}{e} \tan^{-1}\left(e^{-kh/2} \tanh \frac{e_c \psi_p}{4k_B T} \right) \right]^2 \tag{1.13}$$

Figure 14 shows the application of equation(1.12) for the calculation of F_e for two identical latex particles suspended in water. The interaction energy increases with increasing surface potential and decreases with separation distance.

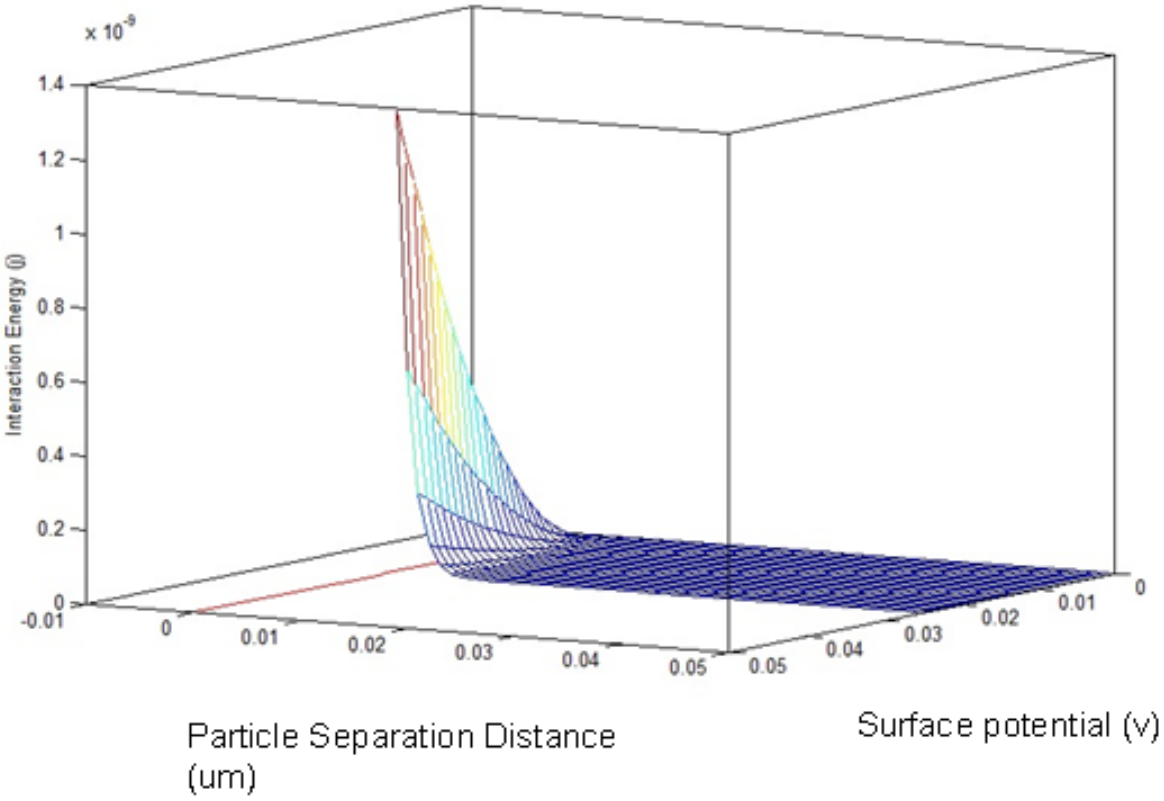

Figure 14 Electrostatic Repulsive Energy for two latex particles of same size for different surface potentials and separation distances

Effect of shear rate on Aggregation

The rate of aggregation depends on a number of parameters such as surface potential, ionic strength, particle size and shear. The effect of shear rate on orthokinetic coagulation is of course, well studied even theoretically. In the absence of electric double-layer repulsion, the collision efficiency varies as –0.18 power of shear rate (see equation 1.15).

There are a number of researchers that have looked into the effect of shear on the aggregation rate and collision efficiency(Mumtaz, Hounslow et al. 1997; Agarwal 2002; Vanni and Baldi 2002; Brien 2003). Vanni looked at two scenarios for a water polystyrene system, the fast coagulation regime where the electrical double layer interactions could be ignored and the slow coagulation regime, where there was strong electrostatic destabilization(Vanni and Baldi 2002). In the first case they found a power law dependence of collision efficiency on particle size and shear rate where in the second case coagulation depended on surface potential and ionic strength but not on shear rate and particle size. Mumtaz found that aggregation rate initially increases with shear rate, hits a maximum and then decreases at high shear(Mumtaz, Hounslow et al. 1997).

In general it has been observed that aggregation rate increases at low shear rates. This can be attributed to the fact that shear is directly proportional to the collision rate and so having higher number of collisions increases the likelihood of aggregation .When shear gets high enough it causes both aggregation and deaggregation causing the aggregation rate to peak. Even though the collision rate continues to increase, the collision efficiency decreases as not all particles are able to stay together after collision due to the hydrodynamic drag acting on them.. At even higher shear the aggregation rate drops sharply and reduces to zero. However it has been noticed that this dependency on shear is specific to the system being studied and the relationship varies dramatically from paper to paper.

Drop formation in an inkjet print head is a function of the flow rate and the surface tension. There are critical values of these parameters at which the drop will separate from the nozzle. They also determine the volume of the drop. Thus to model the drop formation process we need to calculate these parameters. The geometry of a solenoid based inkjet print head is a long thin micro fluidic channel. We assume the flow through channel is a case simple shear flow based on Poiseuille law (Figure 15):

$$\Delta P = \frac{8\mu L Q}{\pi r^4} \quad (1.14)$$

Where ΔP is the pressure drop, L is the length of the channel, μ is the dynamic viscosity of the fluid, Q is the volumetric flow rate and r is the radius of the channel. The typical values for nozzle diameters lie in the range of 100 microns (reference). We can use equation (1.14) to calculate Q as a function of fluid viscosity.

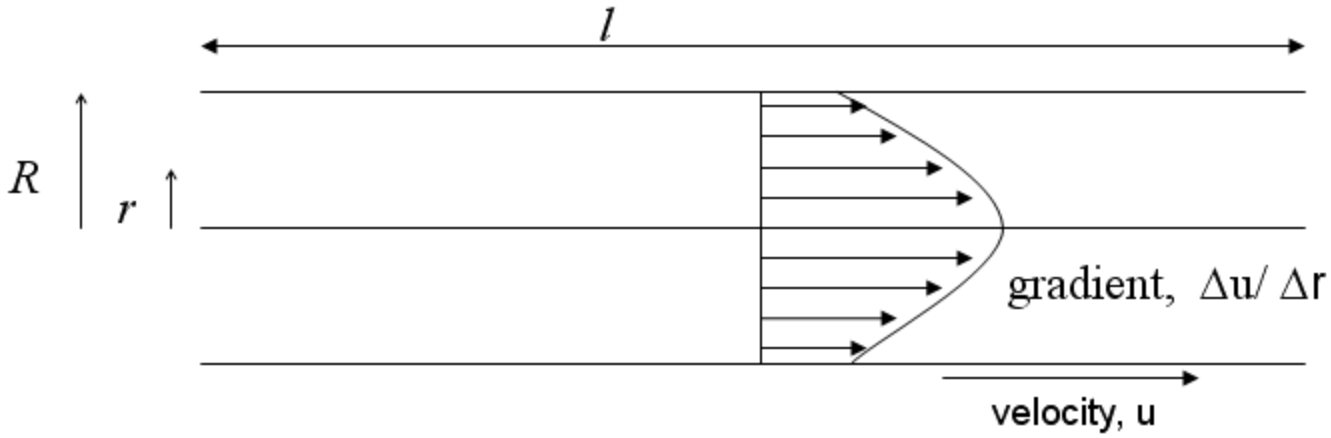

Figure 15Poiseuille Flow in a Cylindrical Nozzle

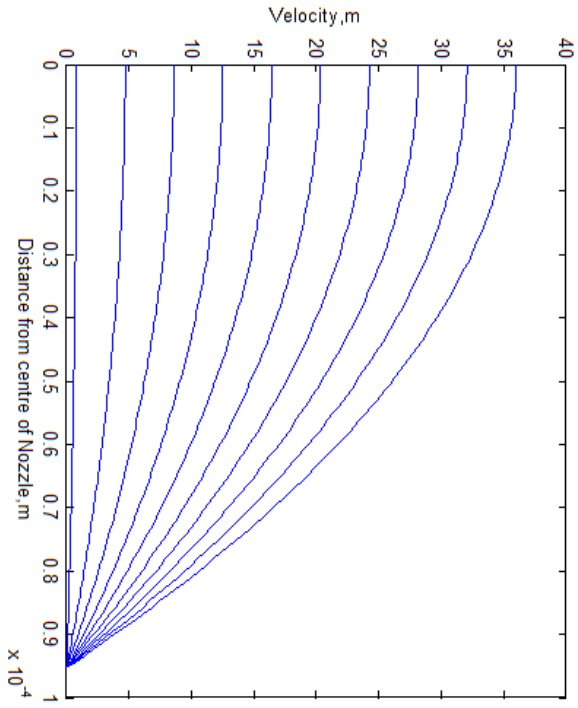

Figure 16 Flow Profile

Also the shear rate can be related to the Reynolds's number. The velocity profile though the pipe is given by the expression:

$$u(r) = \frac{1}{4\mu}\frac{\Delta P}{\Delta x}(R_0{}^2 - r^2) \qquad (1.15)$$

Where μ is the flow velocity, ΔP is the pressure drop, Δx is length of nozzle (L) and R_0 is the radius of the pipe. The shear rate τ, which is directly proportional to the velocity gradient, is given by:

$$\boldsymbol{\tau} = \frac{du}{dr} \qquad (1.16)$$

$$\boldsymbol{\tau} = -\frac{1}{2}\frac{\mathrm{Pr}}{\mu L} \qquad (1.17)$$

We can also find out the average velocity for the flow which is the average velocity of all the particles in a unit cross-section of the tube. So if we integrate from 0 to R, we get total velocity of all the particles and hence dividing the expression by area gives us the average velocity:

$$u_{avg} = \frac{1}{6}\frac{PR_o^{\,2}}{\mu L} \quad (1.18)$$

Finally, to calculate Reynolds's number:

$$R_{ey} = \frac{2u_{avg}R_o}{\eta} \quad (1.19)$$

Where n is the kinematic viscosity. Substituting (1.18) in (1.19) we get:

$$R_{ey} = \frac{1}{3}\frac{PR_0^{\,3}}{\mu\eta L} \quad (1.20)$$

In the case of the solenoid valve we have another method to calculate Reynolds number based on Lohms law for liquids(Ref):

$$Lohms = \frac{KV}{Q}\sqrt{\frac{P}{S}} \quad (1.21)$$

where V is the viscosity correction factor, S is the specific gravity and K is a constant for taking care of units. Lohms is a measure of resistance of flow and can be used to specify performance without concern for coefficients for discharge, passageway geometrics, physical dimensions or tolerances. From Q we can calculate the average velocity and with that, Reynolds number.

$$u_{avg} = \frac{4Q}{\pi d^2} \quad (1.22)$$

$$R_{ey} = \frac{2ru_{avg}}{\eta} \quad (1.23)$$

Figure 17 shows the variation in Reynolds number as a function of pressure for both Lohms based and Poiseuille based values. The two sets compare reasonably well within the range of applied pressure. Thus, our assumption that the flow inside is a laminar Poiseuille flow holds.

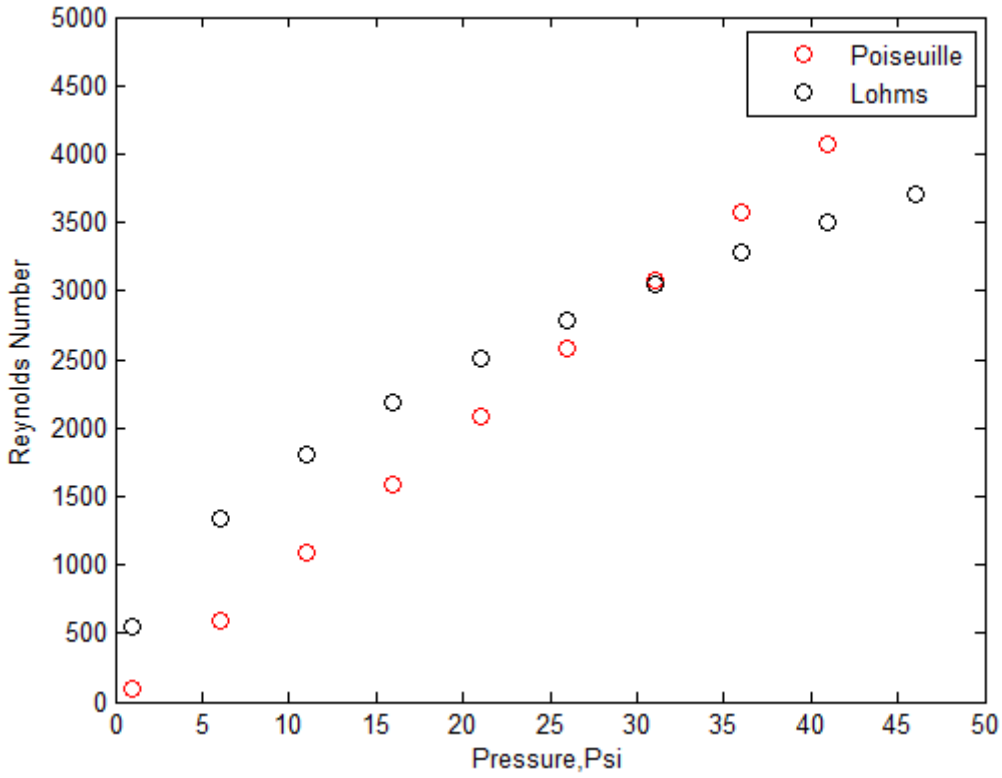

Figure 17 Variation of Reynolds Number as a function of Pressure for Poiseuille Flow (Red) and Lohms (black)

Quantity	unit
Pressure	Pascal

Dynamic Viscosity	Pas
Kinematic Viscosity	m2s-1
Density	Kgm-3
Pipe Radius	m
Reynolds Number	NA
Flow Velocity	ms-1

Table 1 List of terms used

Shear and Aggregation

Stability under shear can be estimated quite easily using force balance approach.

$$F_S = F_e - F_{disp}$$

Where F_S is the shear induced drag force

$$F_S = 6\pi\eta a^2 G$$

Where G is the shear rate. The system is stable if

$$F_e - F_{disp} - F_S > 0$$

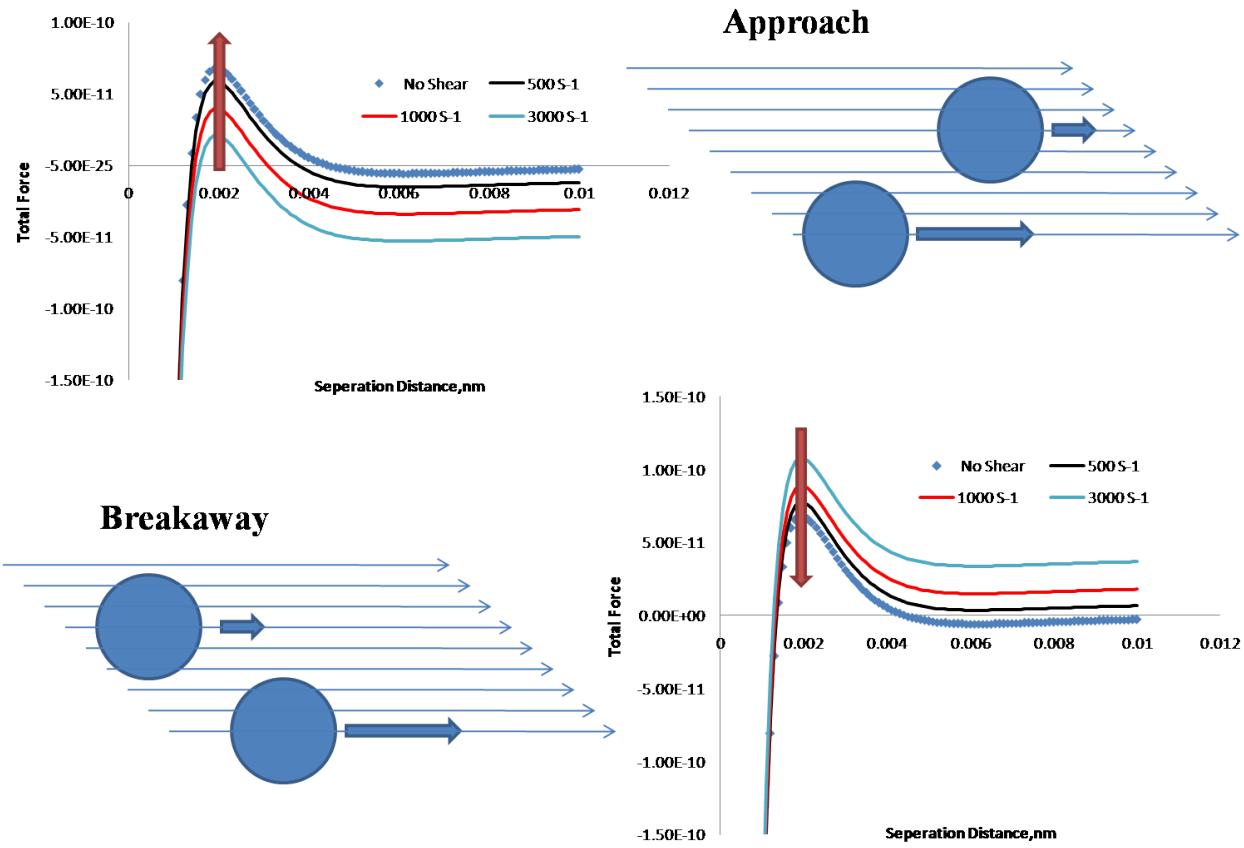

Figure 18 Effect of Shear Force on aggregation behavior: on top we see that during approach of particles drag force adds to the aggregation potential increasing the primary area of stability in the DLVO curve. On the bottom as the particles move away from each other shear acts in an opposite manner

5.1. Material and Methods

Two sets of formulations were prepared .In the first set, 01gm and .02 gm of micronized griseofulvin was mixed into 10 ml of water to prepare .1% and .2% (W/V) suspensions respectively. The formulations were agitated in a vortex mixer to break up the aggregates for 20 seconds. For the second set .1%(w/v) griseofulvin was added to .25%,.5% and 1% (w/v) of HPMC solutions. The formulation was then placed in an ultra sonification unit for 1minute.

5.2. Results

Particle Size was measured before and immediately after dispensing through the system. Figure 19shows the particle size distribution for .1% griseofulvin solution before and after dispensing through the inkjet valve. The nozzle diameter was .005 in and the pressure applied was 10 psi. As we can see the average particle size has slightly increased after being subjected to the forces inside the nozzle. Also the distribution has widened as the peaks are not as sharp.

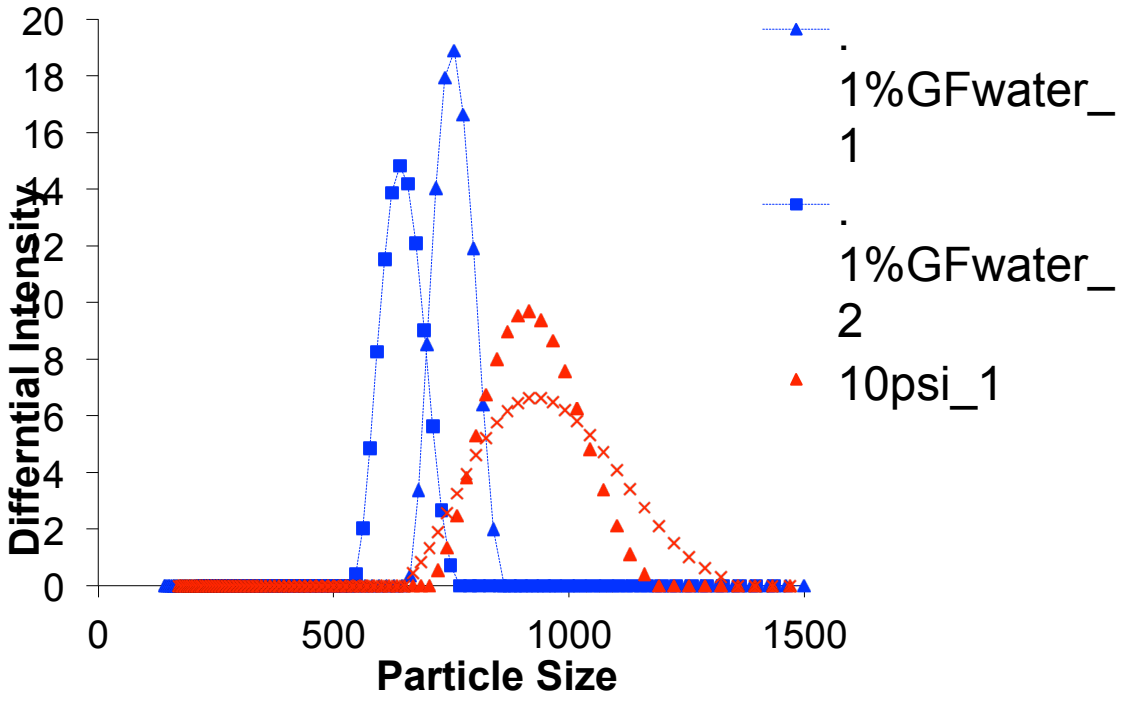

Figure 19Particle Size distribution for .1% griseofulvin suspension in water before (blue) and after (red) dispensing through the system

When we look at the size distributions for HPMC solutions (Figure 20), we see that as the concentration of HPMC increases, the average particle size decreases. When the polymer chains come in contact with griseofulvin particles they adsorb to the surface. When the solution is sonicated the particles de-aggregate but are not able to the aggregate again as the polymer adsorbs on the surface immediately. It follows that more the concentration of polymer the solution, more is the adsorption effect and lesser the particle size.

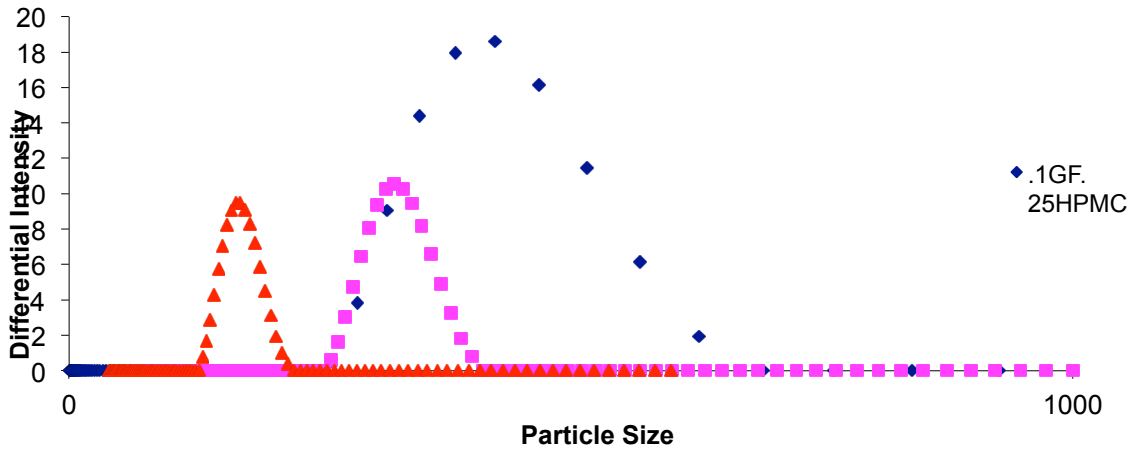

Figure 20 .1% griseofulvin suspension in three different solutions of HPMC (.1% .25% 1%)

6. In Line Analytics

For final dosage form concentration qualification, the emphasis has largely been on Active Pharmaceutical Ingredients (API) by the pharmaceutical industry. The method utilized for dosage control is capsule weighing and we determined the error incurred according to droplet size utilized. However, when a drug is in solution, and more importantly in suspension, other spectroscopic techniques may be more adequate for dosage control. PAT and ICH-Q8 have recognized spectroscopic techniques as useful tools for probing molecular vibrational modes to identify chemical species (Huiquan, Edwin et al. 2008)

This section focuses on Raman spectroscopy, which when coupled with chemometrics, are suitable tools for non-destructive analysis (online and offline) of the contents of powder-filled capsules. For understanding, monitoring and controlling the manufacturing of liquid-filled capsules, we envision the use of these technologies. We foresee their implementation in two manners: One that spectroscopically samples the liquid-filled capsules, as an extension of the methods already developed for solid-filled capsules which are described in a section below. The other implementation method spectroscopically samples the liquid stream (or streams) that fill the capsule. This is expected to present fewer technical challenges than capsule analysis, particularly if the stream contains a single drug (no compound interactions means simpler chemometrics).

Raman

Raman is a promising technique for non-destructive analysis of pharmaceutical solutions because it provides more chemical specificity than NIR. In addition, NIR requires non-parametric multivariate analysis to interpret the data and water provides a huge absorption signal in the IR range, often overwhelming the signals of interest. Raman, on the other hand, allows direct measurement of suspended API concentrations, without the need for knowing the exact volume or density of the sample suspension. Raman has been used to analyze drug composition through packaging (transparent glass, plastics and blisters) (Kim, Chung et al. 2007). Raman has also been used to analyze drugs in suspensions and solutions, in diverse media (ointments, fluids, etc.) (De Beer, Vergote et al. 2004; Rama, Lopez-Sanchez et al. 2005; Mazurek and Szostak 2006; De Beer, Baeyens et al. 2007; Kim, Chung et al. 2007). Raman has been used for quantitative purposes (De Beer, Vergote et al. 2004; Mazurek and Szostak 2006). More importantly for the purpose of online monitoring, there are units such as flow-through sensors that use Raman (Rama, Lopez-Sanchez et al. 2005).

Raman spectroscopy provides a rapid and non-destructive analysis and allows structural fingerprint due to its narrow and highly resolved bands. It is capable of yielding compound-specific information and, as it requires little sample preparation, it allows for real time, on-line analysis.

6.1. Materials and Methods

Materials

In this study we have used Ibuprofen, crystalline powder (> 0.994 %) supplied from Spectrum Chemicals Mfg. Corp, as a model API. Ibuprofen (IB), a 2-arylpropionic acid derivative (Moore 2007) is a chiral non-steroidal anti-inflammatory drug. Ibuprofen is extensively used for postoperative pain, arthritis, injuries and the aches and pains of many illnesses (Davies 1998). Ibuprofen contains a stereo center in the α-position with two possible enantiomers. The $(s)-(+)-$ ibuprofen is the active form but due to the expense involved in making pure $(s)-(+)-$ ibuprofen and the presence of an isomerase in the body, it is sold as a racemic mixture.

Castor oil (Spectrum Chemical Mfg Corp) and carbitol cellosolve (diethylene glycol monoethyl ether, 98%, Alfa Aesar) were used as a solvent. These chemicals are commonly used as excipients for liquid formulations and both are suitable for applications in water-soluble gelatin capsules. The solubility of ibuprofen in carbitol cellosolve was measured to be at least 400 mg/mL, thus allowing us to fill capsules with drug amounts similar to the typical dose of ibuprofen in a tablet. The final formulation contained 30 wt% ibuprofen in a 90:10(wt %) carbitol cellosolve/castor oil mixture.

Capsules

Gelatin capsules have been traditionally used as a dosage format for drugs in solid powder or pellet form. Presently, many of new drug formulations demand filling of liquids into hard gelatin capsules that allows manufacturers to overcome the poor aqueous solubility of API; improve content uniformity of low-dose drugs; and ensure better safety in handling high potency APIs. In the present study we used hard gelatin capsules Licaps^{TM} of size 0 (7.3x21.7 mm) that were obtained from Capsugel (Colmar, France).

Methods

The monitoring system can be placed in two positions; in the supply line or at the target capsule.

Figure 15 shows the schematics of the system incorporated with a Raman monitoring system and the placement of the laser. The concentrations at the two positions are related as the integral of the concentration in the supply line will give the concentration in the capsule.

There are several design questions that need to be answered such as the effect of flow rate if the Raman is added ‘in supply line’ or the height of the laser for application at ‘target capsule’. A number of experiments were conducted to answer these questions.

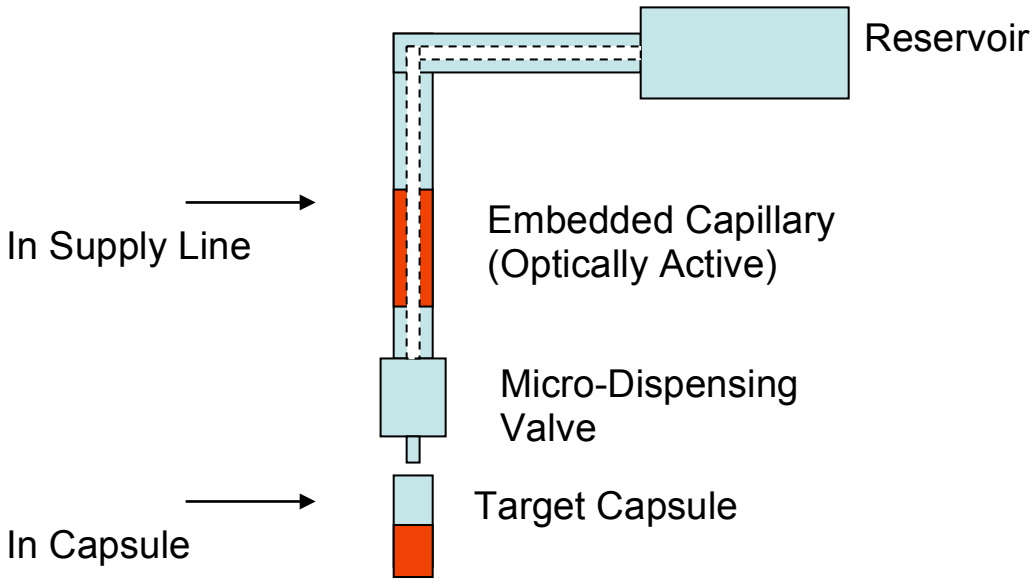

Figure 21 Schematic for In Line Control

Raman: In Capsule

There are three major configurations depicted in Figure 22that differ in the way that laser beam hits the sample, propagates within tested materials and collected by the spectrometer.

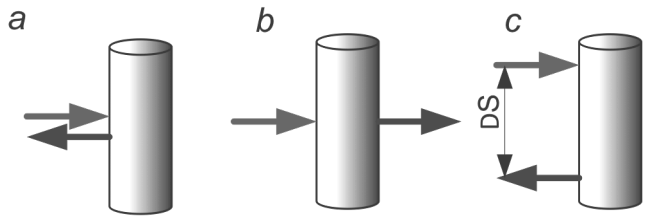

Figure 22 Basic configurations of Raman spectroscopic set-ups with respect to the capsule sample.

External reflectance Raman spectroscopy (ERRS) is a conventional backscattering method for Raman analysis. As shown in Figure 22a laser is placed in front of the sample and scattered light from the illuminated sampling volume is collected. This configuration has been successfully applied to detect drugs in low concentrations (<1%) and to determine API in solid form (Niemczyk, Delgado-Lopez et al. 1998; Mazurek and Szostak 2008). Sample inhomogeneity may be a large source of error when building predictive quantitative methods (Niemczyk, Delgado-Lopez et al. 1998); however, several researchers have successfully applied ERRS configuration to characterize pharmaceutically relevant systems (Niemczyk, Delgado-Lopez et al. 1998; Taylor and Langkilde 2000; Severdia and Siek 2002; Kim, Noh et al. 2007; Mazurek and Szostak 2008).

Transmission mode Raman spectroscopy (TMRS): This method generally overcomes the problems of reflectance methods. It yields the average concentration in the capsule and it has been successfully used to analyze the solid contents of several types of capsules and drugs (Matousek and Parker 2007; Eliasson, Macleod et al. 2008). It has also been used to build quantitative methods for analysis of API formulations (Johansson, Sparen et al. 2007; Eliasson, Macleod et al. 2008).

Spatially offset Raman spectroscopy (SORS): The method is based on the collection of Raman spectra from spatially offset regions away from the point of illumination on the

sample surface (Matousek, Clark et al. 2005). The laterally offset Raman spectra contain different relative contributions from sample layers located at different depths (see Figure 22c). Spatially offset Raman spectroscopy has shown a substantially higher degree of sensitivity in this application area than conventional Raman spectroscopy, primarily because of its ability to effectively suppress Raman and fluorescence contributions from the packaging [(Eliasson and Matousek 2007)].

6.2. Results

Raman: In Stream

The same geometries that apply to capsule-based measurements apply to the detection of API in the supply line of the dispensing system. An optically active capillary or flow cell is placed into the supply line.

Backscattering (in capillary)

The supply line was simulated using an optically active glass capillary (Figure 23). A motorized syringe pump was used to create flow. The exposure time was increased in order to compensate for the reduced scattering from the capillary. The spectrum was measured as the average of five accumulations with a one second exposure time. This was repeated five times for each sample.

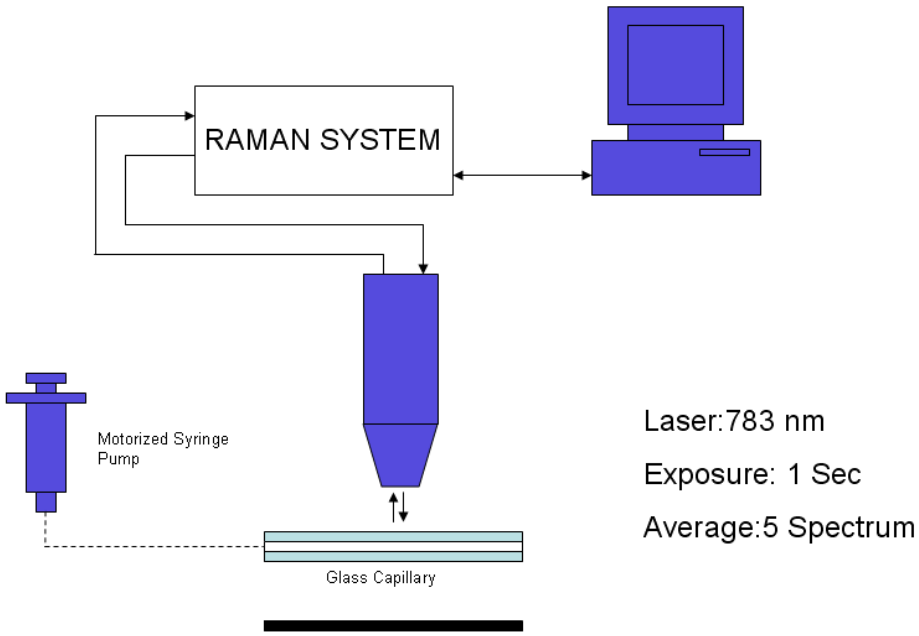

Figure 23 Schematics for backscattering mode in capillary

The spectra were measured for different formulation flow rates through the capillary. Change in flow rate did not produce a significant effect on the Raman spectra (Figure 24). Therefore, this mode of operation is suitable for inline monitoring. In practice, a section of the supply can be replaced by a length of optically active glass capillary. The intensity of Raman scattering increases with drug concentration at certain wavelengths (Figure 25).

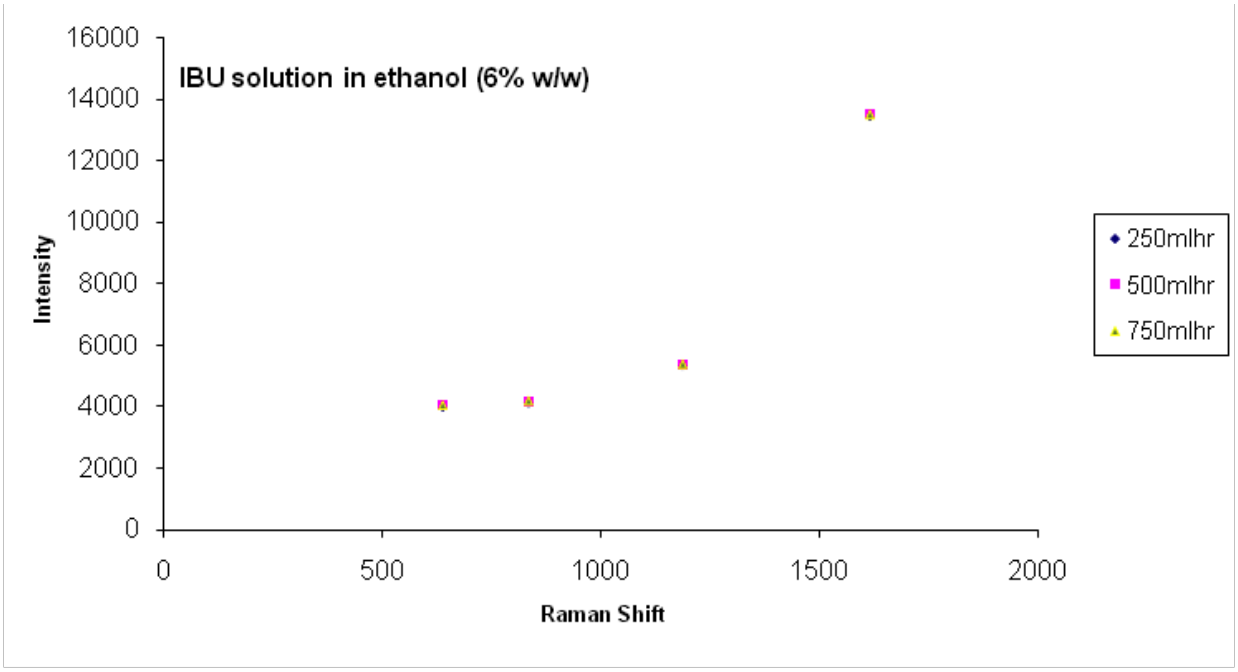

Figure 24 Effect of flow rate on Raman Spectra

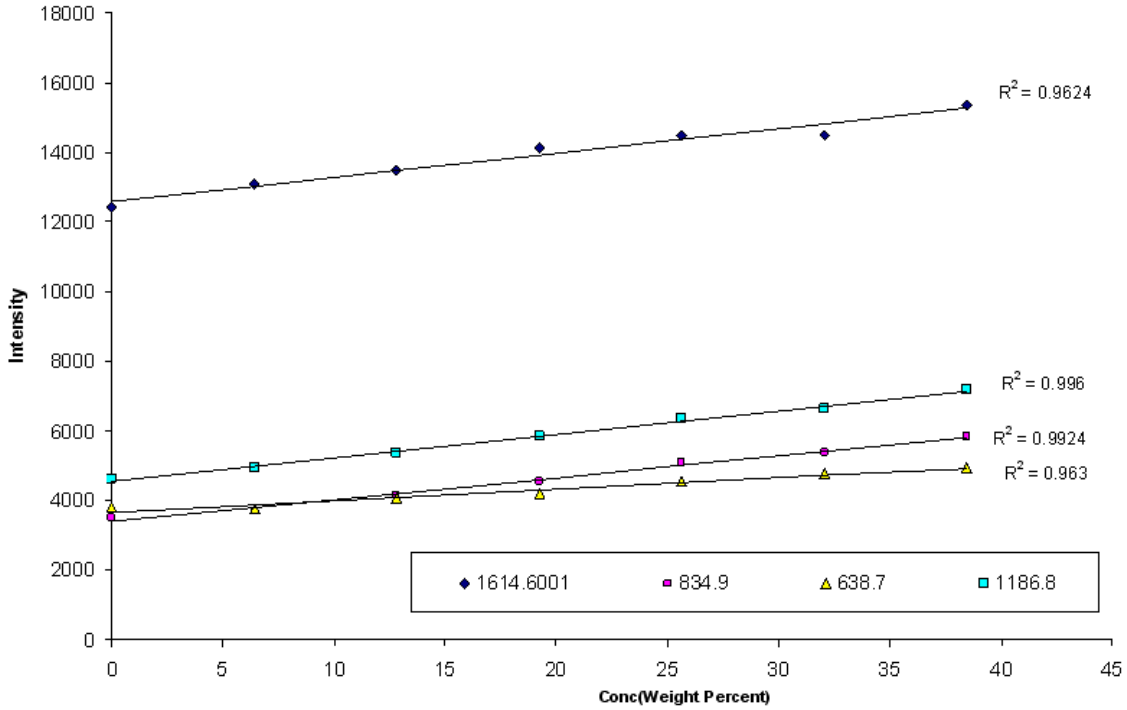

Figure 25 Ibuprofen in ethanol was used to show the increase of intensity with increasing drug concentration for different wavelengths.

Transmission (flow through cell)

For the transmission mode, the drug formulation was pumped through a flow cell containing a very thin capillary. The laser beam is shone through a length of the capillary and the scattered light exiting that length is measured (Figure 26).

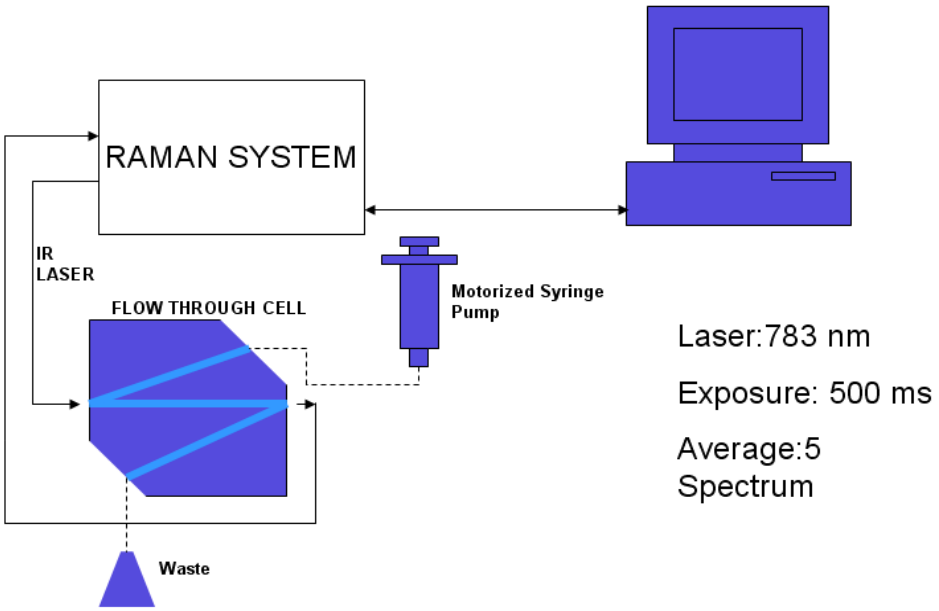

Figure 26 Schematics for Transmission mode

This mode of operation was not very effective for 'in supply line' monitoring of solutions. The optical density of the solutions is low resulting in a higher base level of light scattering masking the Raman scattering. This is indicated by the absence of peaks in the measured spectra. The exposure time was increased to increase level of Raman scattering; however, this did not have a significant effect (Figure 27).

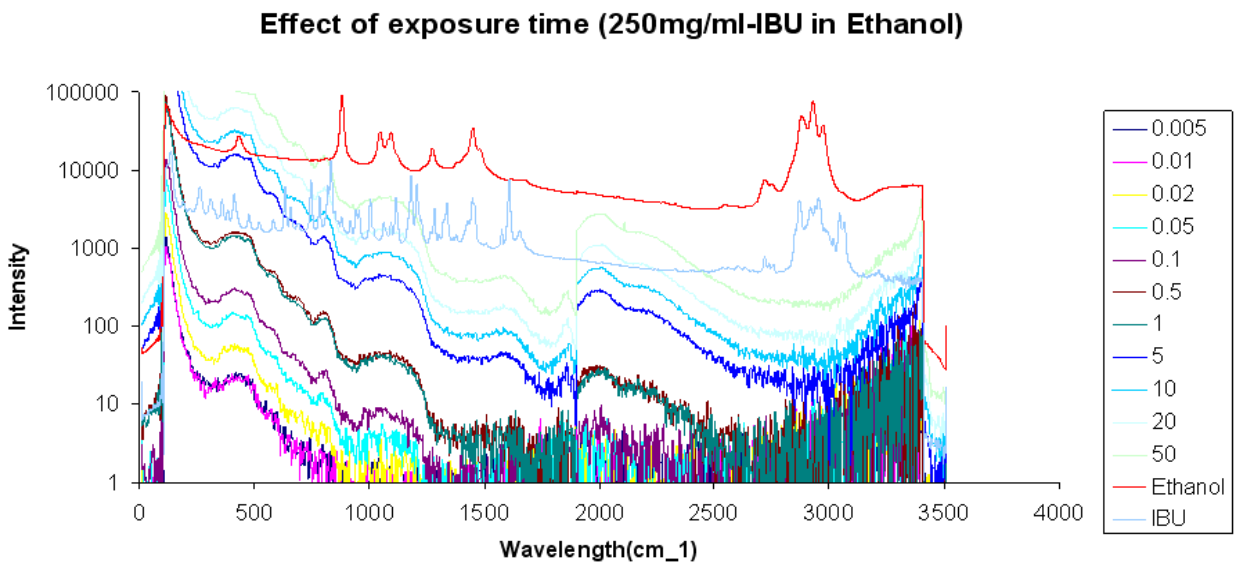

Figure 27 Spectral data for solution from transmission mode compared to standard spectra of pure materials (Ibuprofen and ethanol). The graph shows spectral changes with respect to exposure time

Backscattering (in capsule)

After a capsule was filled with the drug formulation it was placed inside of a standard cell, a black box housing the laser and sample (Figure 28). Parameters such as exposure time and focusing length were chosen to result in the maximum spectra intensity. The spectrum was measured as the average of five accumulations with a 500 ms exposure time. This was repeated five times for each capsule.

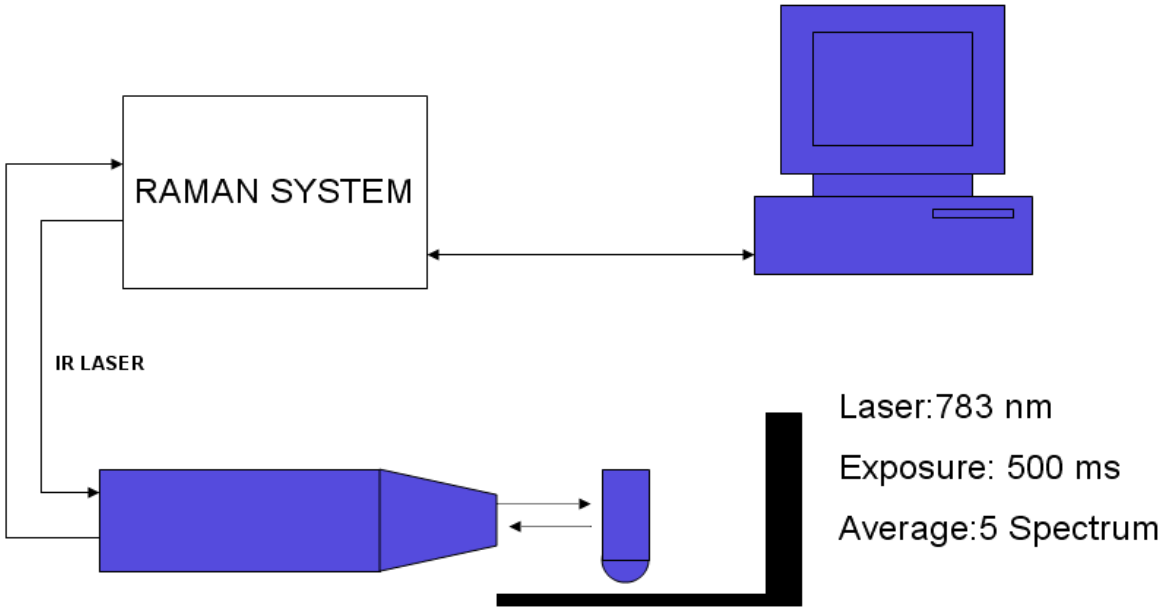

Figure 28 Schematics for back scattering mode for detection in capsule

ERRS detection of Ibuprofen in filled capsule

In order to identify the proper API specific band for the further analysis, Raman spectra were collected from pure crystalline Ibuprofen samples and compared with theoretically predicted Raman spectra (Smith, Stambaugh et al. 2009). Raman band assignment (Table 2Ibuprofen associated Raman bands assignment obtained from DFT calculations and experimentally was performed with KnowItAll software package (Bio-Rad, USA).

Measured Raman peaks of crystalline IB	Theoretically predicted (DFT) Raman peaks	Associated conformational changes in IB molecule
632	638	Ring deformation/COOH scissor
743	729	CH bend (out plane)
779	790	OCO/CH/CC bend
816	817	OCO bend/CH bend/CC bend
829	836	CH bend (out plane)
875	859	CH bend

Measured Raman peaks of crystalline IB	Theoretically predicted (DFT) Raman peaks	Associated conformational changes in IB molecule
915	915	CH bend
945	948	CH bend (out plane)
1003	998	CH bend
1065	1061	CH bend
1112	1118	CH bend/OH bend
1178	1180	CH bend/OH bend
1203	1197	CH bend
1280	1258	CH bend/OH bend
1320	1319	CH bend
1450	1448	CH bend
1608	1589	Ring stretch
1680	1746	OCO(as)/OH bend

Table 2Ibuprofen associated Raman bands assignment obtained from DFT calculations and experimentally

The selection of the bands for the study was determined for the following objectives. First, there is strong background signal due to the presence of the solvents in model drug formulation. The principle of superposition and Beer's law dictate that the intensity of the Raman spectrum at each wave number would be a sum of the each component. Therefore, we need to choose bands for Ibuprofen that did not overlap with the corresponding bands of these compounds. Figure 29 shows the spectra for ibuprofen and solvents used in our experiments. It is clear that some of the solvent bands superimpose on ibuprofen peaks.

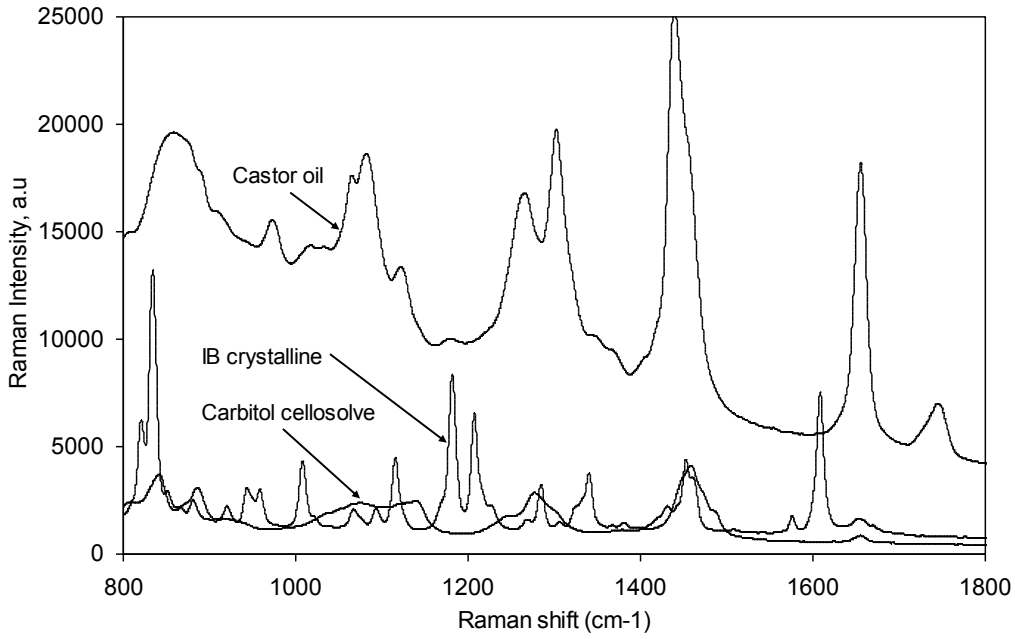

Figure 29 Raman Spectra for Ibuprofen powder, ethanol and castor oil

Figure 30 shows the Raman spectra of ibuprofen in the 800-1800cm^{-1} region. Gelatin blocks a large portion of the Raman scattering. We have to minimize the effect of the capsule material on the resulting spectrum, by choosing API's characteristic bands that have a better signal to noise ratio. From the figure we observe that the only Raman band of crystalline ibuprofen that does not overlap with the bands from the solvents and gelatin is 1608 cm^{-1}. The intensity of this band is relatively high, so it can be used for quantitative analysis as reported in the literature (Breitenbach, Schrof et al. 1999).

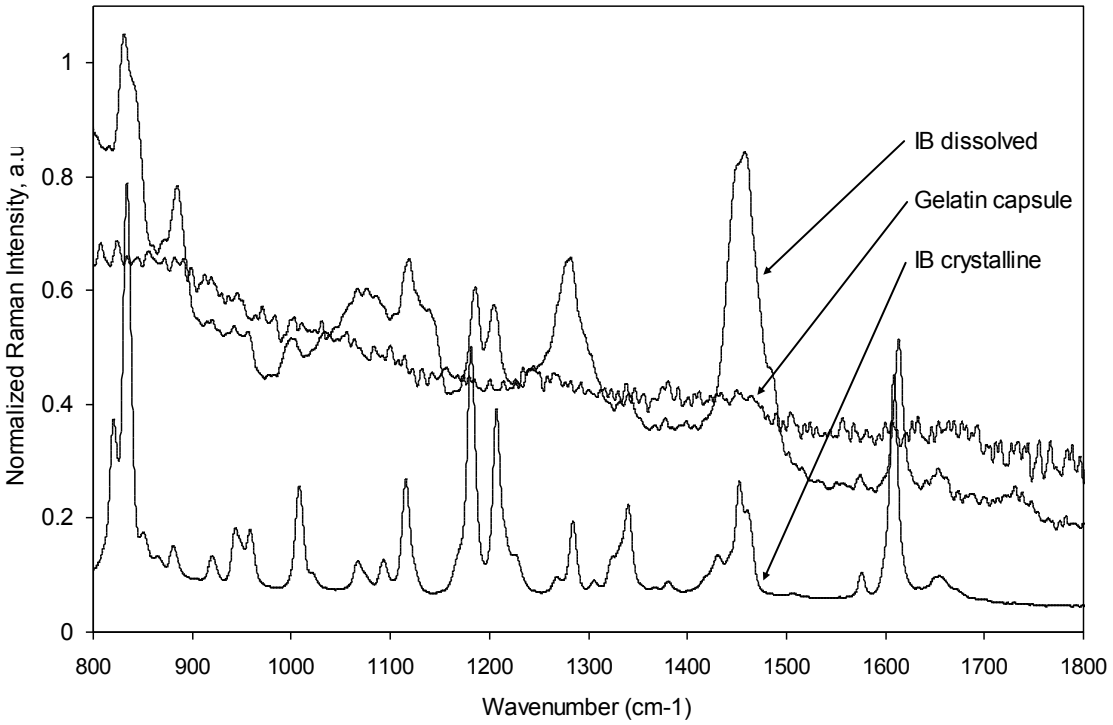

Figure 30 Comparative Raman spectra crystalline drug in powder form, API solution, and un-filled capsule.

In the fingerprint region the Raman band of ibuprofen solution is shifted compared to crystalline ibuprofen (Figure 31). Ibuprofen powder is in crystalline form whereas in solution it is in amorphous form. When we compare the spectra of the powder and the solution between the 1590 cm-1 to 1630 cm-1 we can spot differences. Crystalline Ibuprofen has a carbon ring stretching peak at 1608 cm-1 while that of amorphous Ibuprofen appears at 1614 cm-1. A frequency position shift towards high wave numbers indicates a stiffening of molecular motions(Jubert, Legarto et al. 2006). The band is also broader for amorphous Ibuprofen when compared to crystalline powder form. Breitenbach etc.(Breitenbach, Schrof et al. 1999) have also used this fingerprint region to

distinguish between the two forms. During this experiment we utilize ibuprofen in solution and chose the 1614 cm−1 peak for all our experiments.

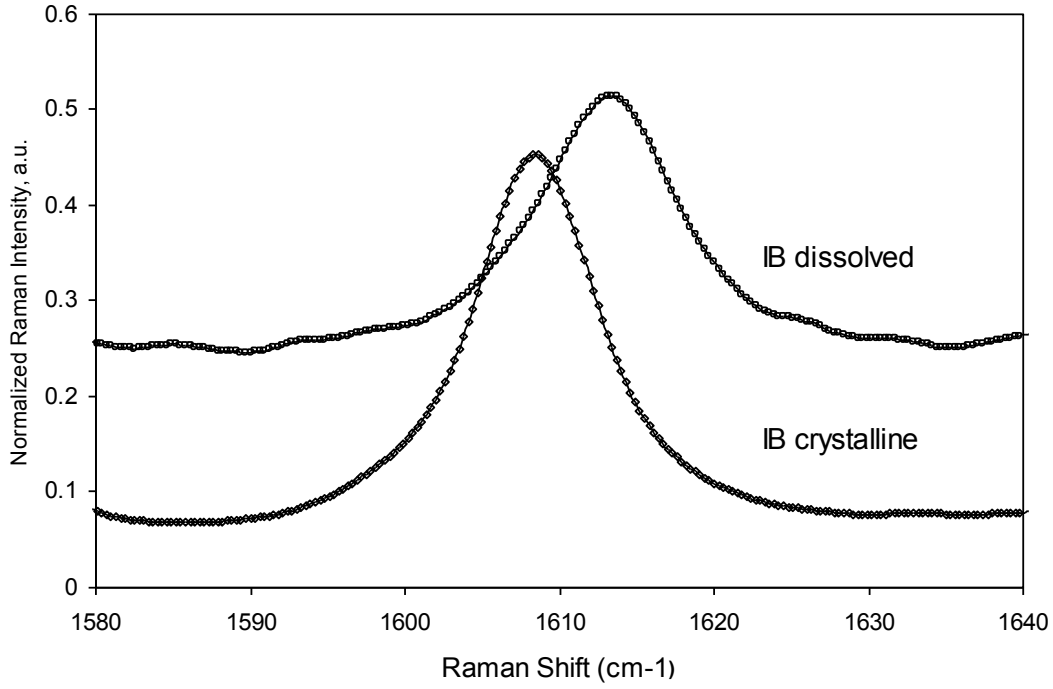

Figure 31 Shift of Raman spectra of ibuprofen in the region of the band at 1600 cm−1.

Five reference standard solutions were prepared with solvent mixture. Calibration samples spanned an adequate concentration range for the API (0…250 mg/ml) and their spectra were recorded with a Raman RXN1 system (see Figure 32). Each spectrum was the average of 5 scans obtained at 500 ms exposure time over the wave number range of 1000…1800 cm^{-1}. Backscattering spectra for samples were obtained in triplicate by filling three capsules with API solution for each concentration

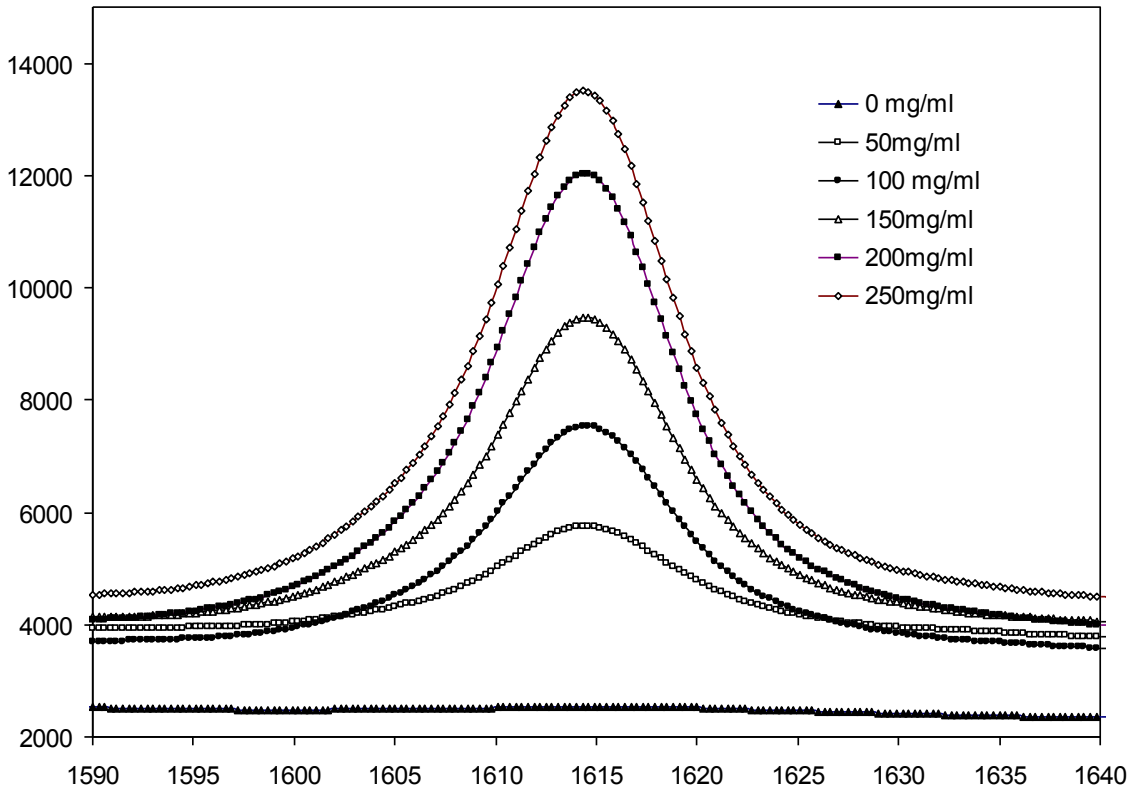

Figure 32 Raman spectra of hard gelatin capsule filled with Ibuprofen solutions at various concentrations

The intensity values at 1614.3 cm^{-1} were selected as the characteristic band for ibuprofen with scattering or fluorescence from solvent or capsule. Equations from the linear model were used to calculate parameter estimates of the calibration model and are shown in Table 3

The adequacy of the model can be tested by evaluating the correlation coefficient; however, we need to test the residuals also, since a value of R close to unity does not necessarily predict a linear calibration function and can lead to misinterpretation.

y=ax+b	a	b
Parameter estimates	189.9	2901.9
Standard error in estimates	α_σ=1.32	β_σ=1.32
σ	448.36	
R^2	0.987	
R^2_{adj}	0.986	
SSR	2.43×10^8	

Table 3 Parameter estimates and statistics for Ibuprofen data

Table 3 displays that both R^2 and adjusted R^2 are close to unity so that our first criterion for fitness is satisfied. Our analysis shows that the residuals are randomly distributed which signifies a good fit to the model (data not shown). Calibration curve and experimental data are in very good agreement as depicted in Figure 33.

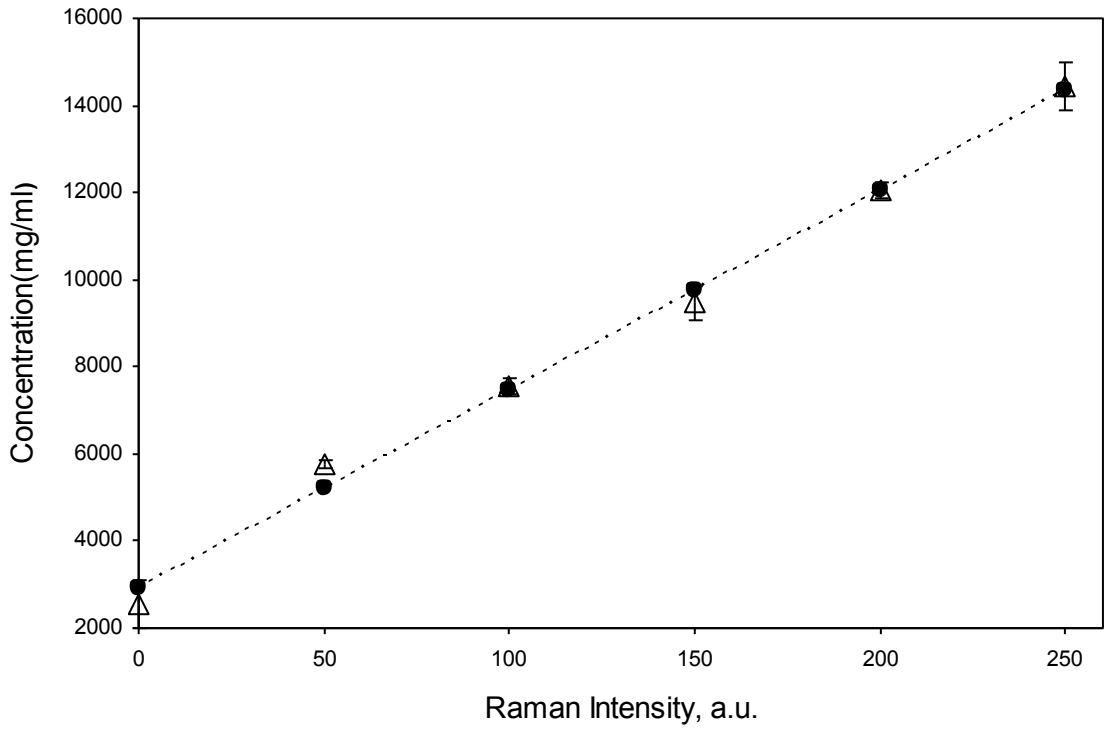

Figure 33 Resulting calibration with ordinary least square regression: measured Raman intensity from the API (△) and predicted values of the Raman signal (○)

The Raman spectroscopic method was validated using UV/Vis spectroscopy, a wet chemistry method. A calibration curve is created from both the Raman and UV/Vis spectroscopic methods. Since each calibration curve represents a linear relationship between concentration and the intensity, the intensity measurement of each method can be directly compared. A linear relationship between the intensities validates the methods.

Solutions of 0, 10, 15, 20, 25, and 30 wt% ibuprofen in a 90:10 mixture of carbitol cellosolve and castor oil were dispensed into capsules. The Raman spectra of each capsule were taken. The calibration curve was created at 1614.6 nm. The capsules were

then dissolved in a USP dissolution apparatus and the UV/Vis spectra measured. The calibration curve was created at 272.6 nm. The intensities of each method at each concentration were then directly compared (Figure 34). The linearity shows that the Raman method is validated by the UV/Vis method.

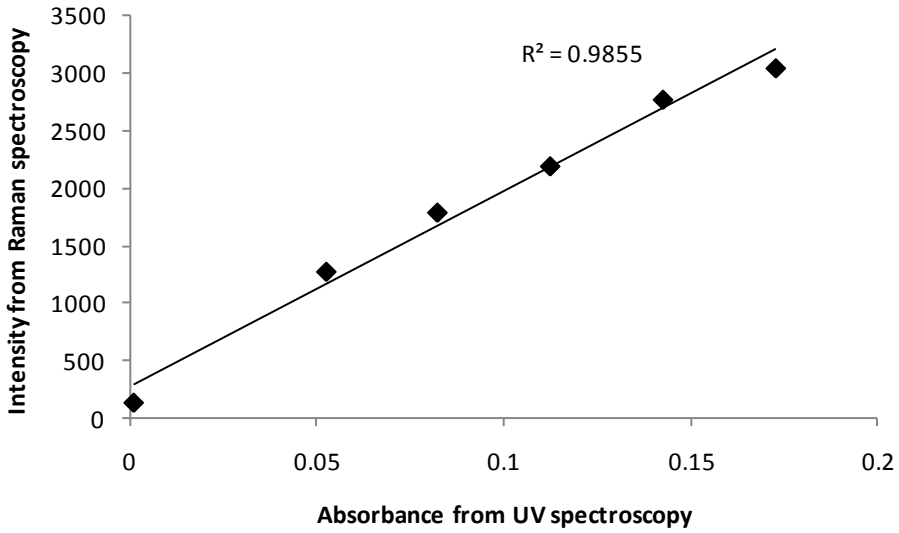

Figure 34 Linearity shows validation of the Raman spectroscopy using UV spectroscopy for solutions.

When the same was attempted for the indomethacin suspension case formulation challenges were met. The difficulty with the Raman spectroscopy was that there was no clear drug peak that was not interfered with by the media peaks. A wavelength of 1690.2 was chosen as the most promising. The calibration curve created at this wavelength was linear indicating that this can be used to determine the concentration of indomethacin inside of the capsule (Figure 35).

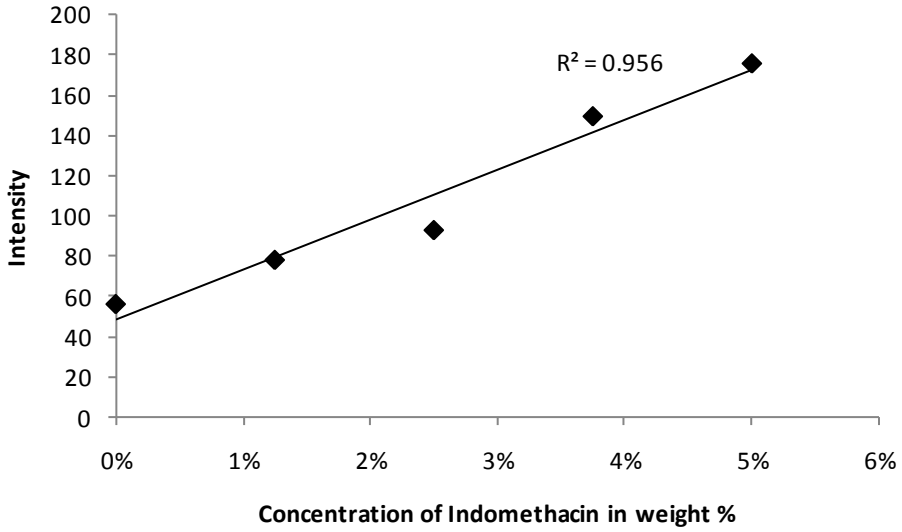

Figure 35 Indomethacin suspension Raman spectroscopy calibration curve.

The application of Raman spectroscopy for the detection of API in suspension requires further development.

6.3. Optimization of Raman probe position regarding the capsule

In order to determine the optimal focusing distance, the laser was placed with the beam spot focused at the center of the filled capsule. Raman probe, which was fixed with clamps on a sliding base, was moved from 0mm to 20 mm with a step size of 2.5 mm. We have approximated spectral response at characteristic band with the 5th order polynomial function $I(\lambda, x) = f(x)\big|_{\lambda=1614}$, where x is the scanning distance. We have used the first derivative test to examine monotonicity properties of obtained polynomial function. Since the derivative of a function changes sign around a critical point ($f'(x) = 0$) we have found a local extremum of the dataset. The derivative of approximating polynomial changes from positive to negative which shows that the function has a local maximum (and therefore an optimal sample-Raman probe distance) $x_{opt} = 7.2$ mm. The intensity of Raman spectra was highest at that focusing distance and the laser was fixed at this point.

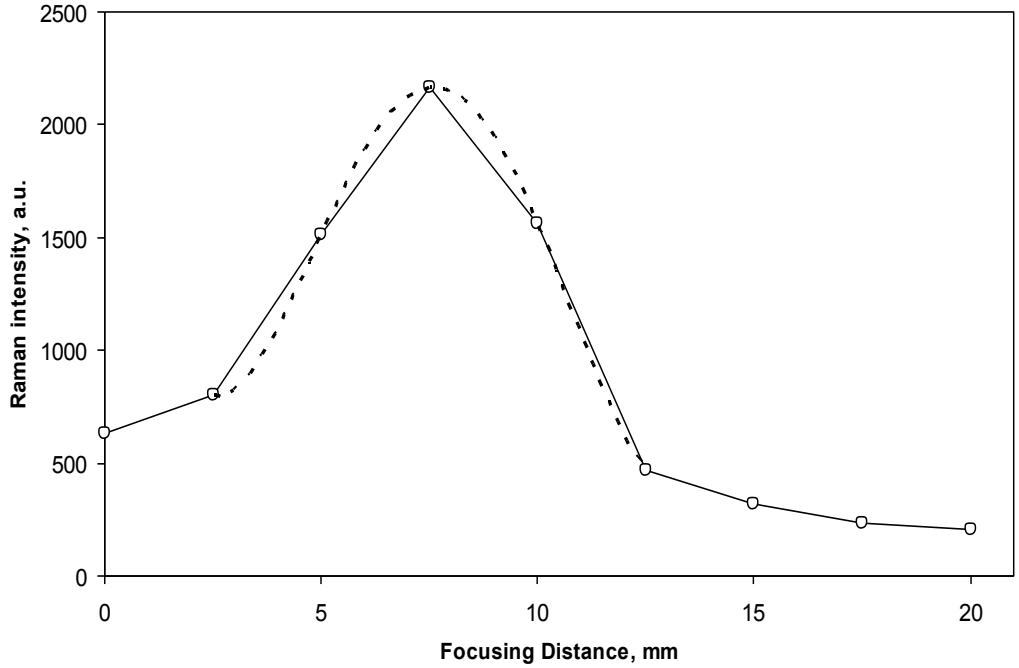

Figure 36 determining of the optimal focusing distance foe the Raman measurement

6.4. Determination of the optimal exposure time

Exposure time is the time for which the data is collected. With the focusing distance fixed, multiple exposure times were checked with 5 replicates each. The objective was to determine the minimum exposure time that can be used without causing a drop in the accuracy of data collected. At each exposure time five replicates were collected and relative standard deviation (RSD) was calculated. For instance, if desired RSD is equal to 1% then minimum exposure time that could be used is about 200 ms.

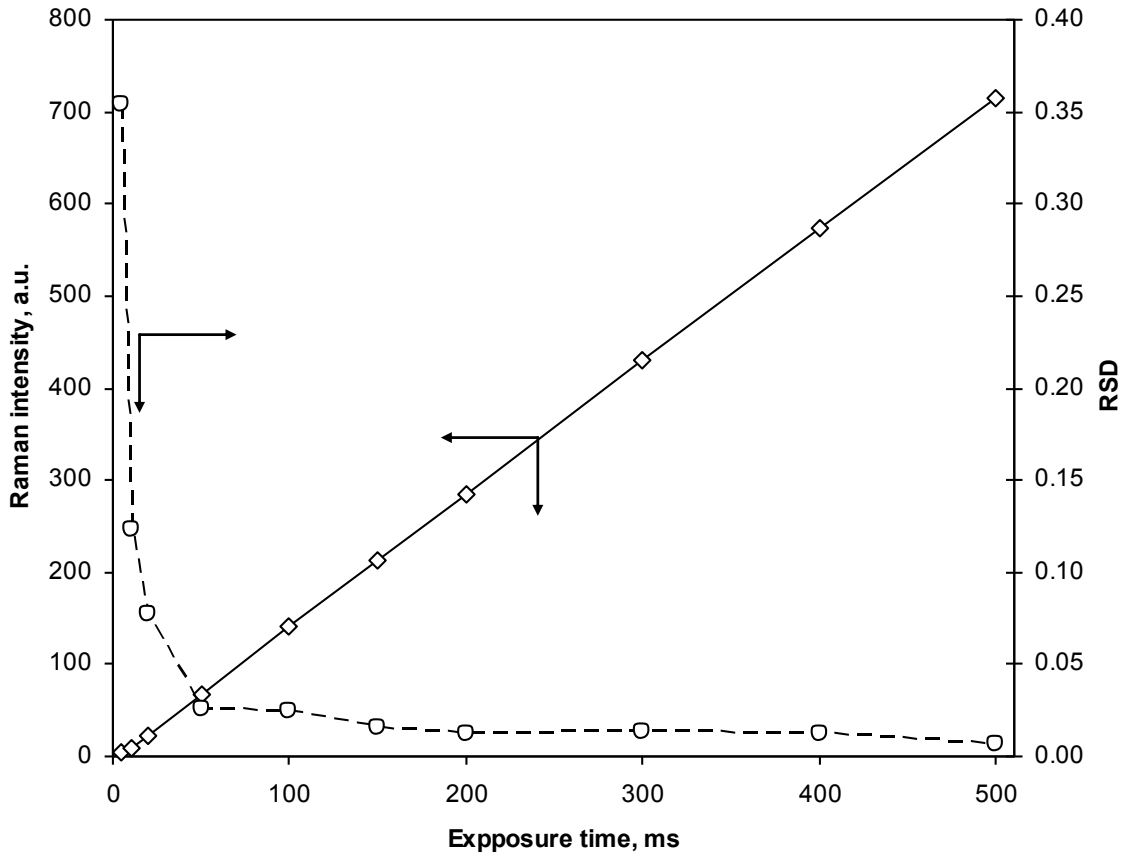

Figure 37 Determining optimal exposure time

6.5. Capsule filling process: analytical considerations

In a scenario where the capsules are getting filled and moving away on an automated tray/line (as depicted in Figure 38) there is a small window of time during which the data can be acquired. This is dependent on the geometry of the capsule and the laser exposure time.

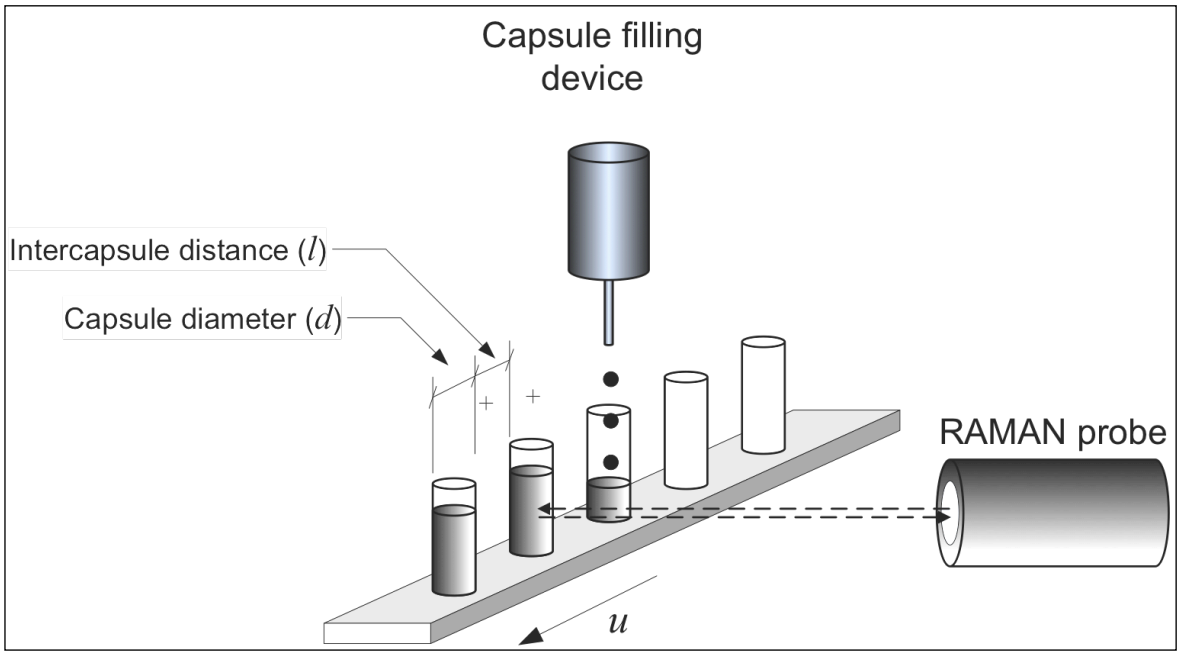

Figure 38 Simplified schematics of the capsule filling process with on-line Raman measurements

Due to cylindrical shape of the capsule it is expected that only part of the capsule diameter (d) will be available for the scanning purpose. Effective scanning length ($d_{eff} < d$) depends on capsule diameter (radius of curvature), thickness of the capsule walls and refractive indices of capsule material and API. Therefore, maximum speed of the capsule passing the probe can be determined as:

$$u = \frac{d_{eff}}{\tau} \qquad (1)$$

Where τ is the exposure time that determined by the specific Raman system.

Time to evaluate API content (t_c) is determining maximum speed (u) at which the scanned capsule is transported in front of Raman probe. However, to scan the entire capsule we need to take into account both the capsule's diameter and inter-capsule distance (l)

t_c can be estimated using following expression:

$$t_c = \tau \frac{(d + l)}{d_{eff}} \qquad (2)$$

In this study we focus on the case where in-capsule measurements of API content are a limiting step. Therefore, productivity P (capsules/sec) of the capsule-filling line with integrated on-line monitoring of the drug content in each unit dosage can be estimated as the following:

$$P = \frac{d_{eff}}{\tau(d + l)} \qquad (3)$$

The horizontal length over which we can scan on the capsule of size 0 with low deviation in intensity is about 2mm. We have also determined the lowest exposure time without sacrificing accuracy of measurement to be approximately 200 ms. These parameters can be used to find the maximum scan speed (u) for a measurement, which determines the conveyor speed on the assembly line.

Finally if we assume that the distance between the capsules is one half of their diameter (3mm) we find that the minimum scan speed is approximately 1 capsule per second.

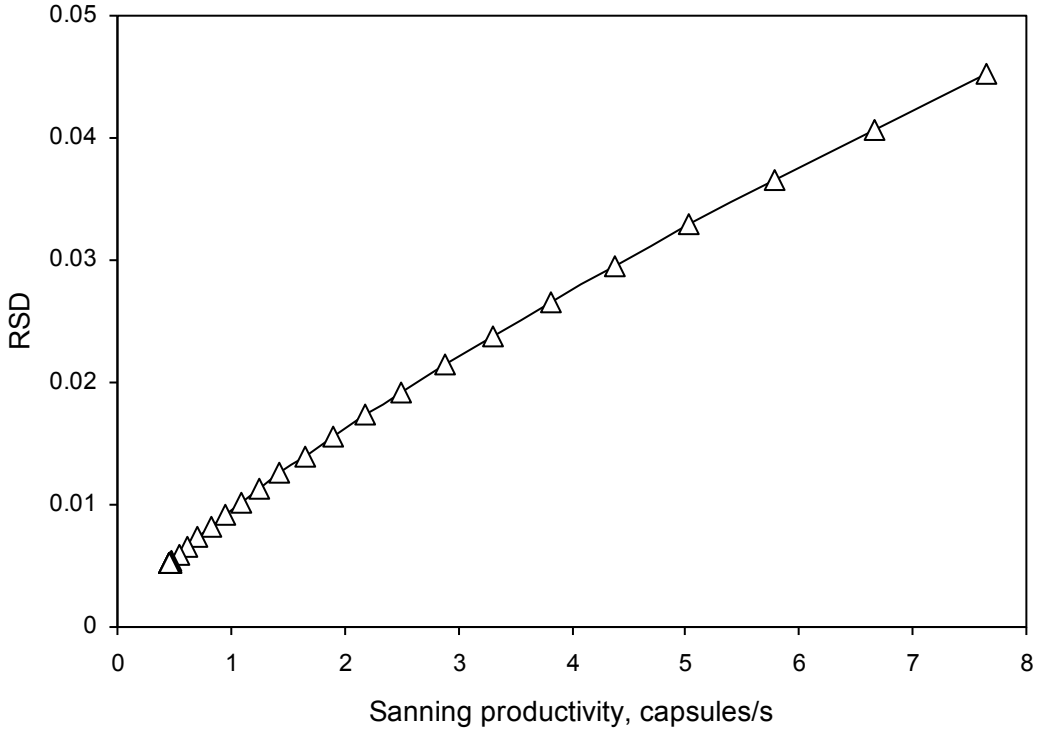

Figure 39 Estimated relative standard deviation of the measured API content as function of the scanning productivity.

Thus by determining the appropriate exposure time we can optimize for number of capsule scanned per minute and increase productivity.

7. Discussion

7.1. Unit dosage application: Filling mode

For a given opening time of the valve, every fluid portion dispensed into receiving container should increase the total mass by a constant value and the WM reading should increase linearly. Therefore, the aliquot reproducibility is assessed by measuring the deviation of the balance recording (total fluid mass versus the number of aliquots dispensed) from a straight line. The results show that, in general, the gravimetric readings fit a straight line with an $R^2 \geq 0.995$

We have assessed an ability of the system to dispense any desired amount of model fluid with the appropriate combination of cycles and opening time of the valve. The opening time of the valve is a critical parameter in the design of a dosage expending protocol. For example, using the system for 100 cycles and different opening times of the valve, a correlation between the latter and the fluid mass dispensed can be established. Our data shows that the mass of water dispensed after 100 cycles increases linearly with the time used for the opening of the valve. The correlation between VOT and the fluid mass dispensed in 100 cycles is perfectly linear with $R^2 = 1$ (data not shown). Therefore, it is possible to design micro dispensing operation with the high level of accuracy and reproducibility.

Figure 40 Filling vial with drug formulation via two-nozzle micro dispensing set-up. Pharma-grade coloring agents have been added for visualization purposes

7.2. Unit dosage application: Printing mode

Another application evaluated is the ability of the system to print precise and reproducible amounts drug solutions onto varying substrates (Figure 41 & Figure 42). This ability is necessary in the design of DDS (Drug Delivery System) which entail precision dosing, time-dependent dosing, or other advanced delivery modes, e.g. matrix drug delivery in controlled DDS. In printing mode the system parameters such as opening time of valve (τ), column and row distance, and pressure are manipulated to obtain printed drops of drug solution of desired quality. In order to ensure that the desired product is obtained it is critical that all system parameters are accurate and easily controlled.

There is a potential to print designed ratios of drugs and excipients as individual microdots onto a suitable substrate, each capable of the controlled release of the active from that deposit. Printing of many thousands of such spots with one or more drugs could be used to build up an effective formulation capable of dealing a therapeutic dose.

There are a number of secondary advantages that such an approach would have. As the medicine would be designed to be printed and consumed at the point of care there would be relatively little need to consider the long-term stability of the formulation. Drugs that may have good therapeutic properties can fail to come to the market due to their poor chemical and physical stability, often through complex solid state interactions with other formulation components. In addition, geriatric medicine regimes, which often involve the taking of a significant number of different drugs many times a day, could be combined into a single dosage form with consequent improved patient compliance.

Variation of key parameters of the system enables the production of printed solutions and DDS with desired properties. In some instances reproducibility and accuracy are desired while in other applications droplets with varying properties are produced. Figure 41 depicts drug printing with variations in impingement substrate and/or process parameters.

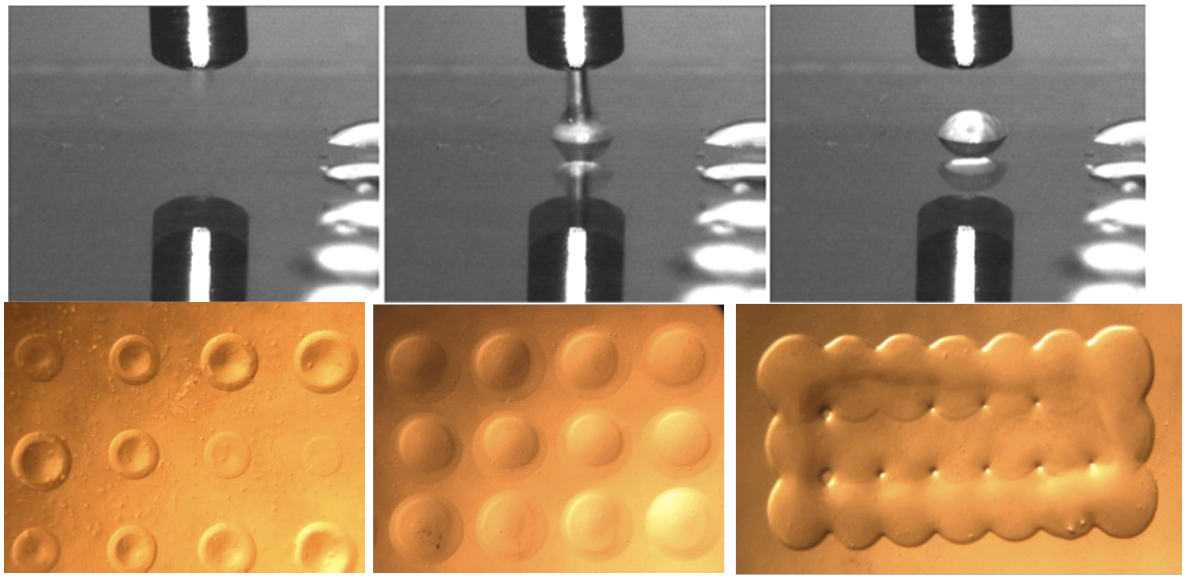

Figure 41 High-speed imaging of the dopamine hydrochloride printing and resulting surfaced patterns produced through manipulation of key process parameters: (a) ramp of variable valve opening times, (b) regular square lattice array pattern, (c) printed array with overlapped API elements

To test the accuracy and robustness of the system two experiments were undertaken. In the first experiment a single drop of dopamine hydrochloride solution was deposited onto a bio-polymeric substrate at increasing tau resulting in increased droplet volume. The droplet diameter at each tau was then measured for 6 trials to determine the robustness and repeatability of the Drop-on-Demand system in printing mode. In the second experiment 25 droplets of approximately 4×10^{-4} ml were deposited simultaneously to measure the droplet weight. The average weight and the standard deviation can be seen in Table 4.

Tau (ms)	*Average Diameter (mm)*	*STDEV*	*Average Weigh t (g)*	*STDEV*
1.00000	1.52357	0.02351	0.00302	0.00008
5.00000	1.80170	0.06417	0.01123	0.00021
10.00000	2.73787	0.10156	0.02029	0.00098
20.00000	2.85996	0.13944	0.03835	0.00087

Table 4 Droplet Diameter and Droplet Weight

We have found that in printing mode the system is robust, precise, and accurate. It enables for the production of advanced drug delivery systems through automation. Varying types of drops utilizing different drug solutions are able to be printed within exact range. Furthermore the system provides increased efficiency and allows for easy adaptation in the printing of different types of drug patterns, droplet diameters, and drug type.

8.

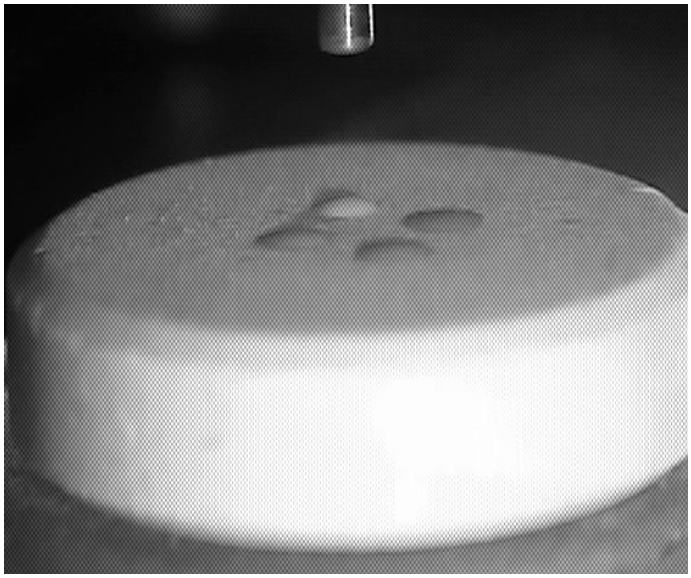

Figure 42 Deposition of API's onto Tablets

8. Conclusion

The need for the development of novel dosage forms and delivery devices for oral individual drug therapy has been well recognized. Various approaches have also been proposed, predominantly in patent literature. However, clinical studies and practical implementation needed to prove the quality and success of these concepts have still not been conducted in adequate measure. The practices that are commonly used are dosing liquids by droppers, spoons and syringes or splitting tablets into segments, but these bear various risks as continuously as reported in literature. Dispensers for multi-particulate dosage forms have been developed but up to now there is only one dispenser for pellets available in the market with minor dosing flexibility. More advanced delivery devices have been proposed, but these have not reached the market most probably due to high costs involved.

Several disadvantages and challenges in the use of inkjet printing in fabrication of drug substances exist. For instance, it is difficult to print high-dose drugs and it remains to be seen how mass production throughputs will meet the needs for large-scale manufacture. Also, comprehensive investigations are still needed for the development of optimal (often biodegradable) substrates, and with regard to printing of more complex dosage forms with multiple drugs and functional coatings. Moreover, the challenges regarding regulatory approval have also to be addressed.

An all-automated method to generate droplets train for filling or printing pharmaceutically relevant solution allows a self-sufficient portable mini-manufacturing platform for customizable dosage formulation. Using this technique could significantly reduce problems, such as drug overdosing, by individually tailoring the drug dose to the constitution, lifestyle and potentially to the genetic profile of the individual patient. Furthermore, by printing time release layers on top of a drug layer, well defined time profiles for controlled drug delivery may also be achieved.

This technique could also help reduce costs in the development of new pharmaceuticals; for instance, for dosing studies during phase I clinical studies, reducing lengthy development times and the problems associated with classical formulation work, as only a solution or dispersion has to be processed. Drugs could be developed faster, thus meeting the goals of the critical path initiative of the FDA, which focuses on methods to speed up pharmaceutical development. Lastly, the technique also provides interesting perspectives for low-dose and multi-dose drugs by providing excellent and verifiable dose accuracy and homogeneity, as well as reducing or even eliminating negative interactions of the individual APIs, as they can be printed at different positions

A major goal of this study was to develop analytical approach for fast and reliable non-destructive assaying of capsule content. This is especially important for non-destructive testing for micro batch manufacturing, clinical trials and personalized therapies, because in such applications the number of product units is typically very small and the burden of

performing destructive tests is proportionally much higher than in large scale manufacturing.

We demonstrated experimentally that backscattering configuration of Raman spectroscopy is well suited for non-destructive on-line probing of pharmaceutical capsules. Raman spectroscopy coupled with chemometrics is a suitable tool for real-time analysis of the contents of liquid-filled hard gelatin capsules. We envision the use of these technologies for understanding, monitoring and controlling the manufacturing of liquid-filled capsules. To our best knowledge, Raman methods have not been used for the analysis of liquid-filled gelatin capsules.

We have successfully designed and implemented hardware and software for the real-time feedback control, in combination with the drop-on-demand generation with solenoid actuation and real-time gravimetric control. The all electrical feedback control system has potential for practical applications. We show the possibility of the generation of varying volumes of droplets on a given pattern in printing mode. Proposed feedback control system parameters and algorithm can be easily programmed with a PC. The former can improve device reliability by compensating for the uncertainties in the dispensing nozzle, dispensing fluid properties and operation conditions, while the latter allows a new flexibility in fluidic operations, such as a high-order solution dilution. More sophisticated and advanced feedback control algorithms, supported by detailed modeling of the nonlinear droplet pinch-off process where still a lot research needs to be done, are

expected to improve convergence speed, stability, system error and robustness of the control system. Through automatic system identification or neural network studies, the feedback controller may be improved in the future to self-calibrate for different solutions and devices without human intervention.

9. List of References

(FDA), F. a. D. A. (2004). PAT Guidance for Industry—A Framework for Innovative Pharmaceutical Development, Manufacturing and Quality Assurance.

Agarwal, S. (2002). Efficiency of Shear-Induced Agglomeration of Particulate Suspensions Subjected to Bridging Flocculation, West Virginia University.

Ancel, H. (2011). Ansel's Pharmaceutical Dosage Forms and Drug Delivery Systems

Breitenbach, J., W. Schrof, et al. (1999). "Confocal Raman-Spectroscopy: Analytical Approach to Solid Dispersions and Mapping of Drugs." Pharmaceutical Research**16**(7): 1109-1113.

Breitenbach, J., W. Schrof, et al. (1999). "Confocal Raman-spectroscopy: analytical approach to solid dispersions and mapping of drugs." Pharm Res**16**(7): 1109-1113.

Brien, C. (2003). A Mathematical Model for Colloidal Aggregation. Department of Chemical Engineering, University of South Florida. **Master of Science**

Davies, N. M. (1998). "Clinical Pharmacokinetics of Ibuprofen: The First 30 Years." Clinical Pharmacokinetics**34**(2): 101-154.

De Beer, T. R. M., W. R. G. Baeyens, et al. (2007). "Influence of particle size on the quantitative determination of salicylic acid in a pharmaceutical ointment using FT-Raman spectroscopy." European Journal of Pharmaceutical Sciences**30**(3-4): 229-235.

De Beer, T. R. M., G. J. Vergote, et al. (2004). "Development and validation of a direct, non-destructive quantitative method for medroxyprogesterone acetate in a pharmaceutical suspension using FT-Raman spectroscopy." European Journal of Pharmaceutical Sciences**23**(4-5): 355-362.

Eggers, J. (1997). "Nonlinear dynamics and breakup of free-surface flows." Reviews of Modern Physics**69**(3): 865.

Eliasson, C., N. A. Macleod, et al. (2008). "Non-invasive quantitative assessment of the content of pharmaceutical capsules using transmission Raman spectroscopy." Journal of Pharmaceutical and Biomedical Analysis**47**(2): 221-229.

Eliasson, C. and P. Matousek (2007). "Noninvasive Authentication of Pharmaceutical Products through Packaging Using Spatially Offset Raman Spectroscopy." Analytical Chemistry**79**(4): 1696-1701.

Furbank, R. J. and J. F. Morris (2004). "An experimental study of particle effects on drop formation." Physics of Fluids**16**(5): 1777-1790.

Gnoth, S., M. Jenzsch, et al. (2007). "Process Analytical Technology (PAT): Batch-to-batch reproducibility of fermentation processes by robust process operational design and control." Journal of Biotechnology**132**(2): 180-186.

Group, W. B. (1998). Pollution Prevention and Abatement Handbook, WORLD BANK GROUP.

Hogg, R., T. W. Healy, et al. (1966). "Mutual coagulation of colloidal dispersions." Transactions of the Faraday Society**62**: 1638-1651.

Hongming, D. (2006). DROP-ON-DEMAND INKJET DROP FORMATION AND DEPOSITIONSchool of Polymer, Textile And Fiber Engineering, Georgia Institute of Technology. **Doctor Of Philosophy**.

Huiquan, W., J. H. Edwin, et al. (2008). "Process analytical technology (PAT): Quantification approaches in terahertz spectroscopy for pharmaceutical application." Journal of Pharmaceutical Sciences**97**(2): 970-984.

Johannes G. Khinast, A. Z., Guenter Brenn, Wolfgang Bauer, Bernhard Eitzinger, Daniela Strohmeier, Nina Schroedl, Michael M. Gruber, Christine Voura (2011). "Printable Medicines: A Microdosing Device For Producing Personalized Medicines." PHARMACEUTICAL TECHNOLOGY EUROPE**23**(1).

Johansson, J., A. Sparen, et al. (2007). "Quantitative transmission Raman spectroscopy of pharmaceutical tablets and capsules." Applied Spectroscopy**61**(11): 1211-1218.

Jubert, A., M. L. Legarto, et al. (2006). "Vibrational and theoretical studies of non-steroidal anti-inflammatory drugs Ibuprofen [2-(4-isobutylphenyl)propionic acid]; Naproxen [6-methoxy-[alpha]-methyl-2-naphthalene acetic acid] and Tolmetin acids [1-methyl-5-(4-methylbenzoyl)-1H-pyrrole-2-acetic acid]." Journal of Molecular Structure**783**(1-3): 34-51.

Kim, J., J. Noh, et al. (2007). "Direct, non-destructive quantitative measurement of an active pharmaceutical ingredient in an intact capsule formulation using Raman spectroscopy." Analytica Chimica Acta**598**(2): 280-285.

Kim, M., H. Chung, et al. (2007). "A new non-invasive, quantitative Raman technique for the determination of an active ingredient in pharmaceutical liquids by direct measurement through a plastic bottle." Analytica Chimica Acta**587**(2): 200-207.

Li, L., M. Saedan, et al. (2009). "Development of a multi-nozzle drop-on-demand system for multi-material dispensing." Journal of Materials Processing Technology**209**(9): 4444-4448.

Lin, S. P. and R. D. Reitz (1998). "Drop and spray formation from a liquid jet." Annual Review of Fluid Mechanics**30**: 85-105.

Lin, S. P. and R. D. Reitz (1998). "DROP AND SPRAY FORMATION FROM A LIQUID JET." Annual Review of Fluid Mechanics**30**(1): 85-105.

Matousek, P., I. Clark, et al. (2005). "Subsurface Probing in Diffusely Scattering Media Using Spatially Offset Raman Spectroscopy." Applied Spectroscopy**59**: 393-400.

Matousek, P. and A. W. Parker (2007). "Non-invasive probing of pharmaceutical capsules using transmission Raman spectroscopy." Journal of Raman Spectroscopy**38**(5): 563-567.

Mazurek, S. and R. Szostak (2006). "Quantitative determination of diclofenac sodium and aminophylline in injection solutions by FT-Raman spectroscopy." Journal of Pharmaceutical and Biomedical Analysis**40**(5): 1235-1242.

Mazurek, S. and R. Szostak (2008). "Quantitative determination of diclofenac sodium in solid dosage forms by FT-Raman spectroscopy." Journal of Pharmaceutical and Biomedical Analysis**48**(3): 814-821.

Moore, N. (2007). "Ibuprofen: a journey from prescription to over-the-counter use." Journal of the Royal Society of Medicine**100**: 2-6.

Mumtaz, H. S., M. J. Hounslow, et al. (1997). "Orthokinetic Aggregation During Precipitation: A Computational Model for Calcium Oxalate Monohydrate." Chemical Engineering Research and Design**75**(2): 152-159.

Niemczyk, T. M., M. M. Delgado-Lopez, et al. (1998). "Quantitative determination of bucindolol concentration in intact gel capsules using Raman spectroscopy." Analytical Chemistry**70**(13): 2762-2765.

Pardeike, J., D. M. Strohmeier, et al. "Nanosuspensions as advanced printing ink for accurate dosing of poorly soluble drugs in personalized medicines." International Journal of Pharmaceutics(0).

Rama, M. J. R., M. Lopez-Sanchez, et al. (2005). "Flow-through sensor with Fourier transform Raman detection for determination of sulfonamides." Analyst**130**(12): 1617-1623.

Rezvanpour, A. and C.-H. Wang (2011). "Computational and experimental studies of electrospray deposition process in pharmaceutical micro-pattern formation." Chemical Engineering Science**66**(17): 3836-3849.

Sader, J. E., S. L. Carnie, et al. (1995). "Accurate Analytic Formulas for the Double-Layer Interaction between Spheres." Journal of Colloid and Interface Science**171**(1): 46-54.

Sandler, N., A. Määttänen, et al. (2011). "Inkjet printing of drug substances and use of porous substrates-towards individualized dosing." Journal of Pharmaceutical Sciences**100**(8): 3386-3395.

Severdia, A. G. and K. Siek (2002). "Fourier transform Raman spectroscopy for identification and differentiation between dosage strengths of an active drug in white opaque hard gelatin capsules." Applied Spectroscopy**56**(4): 545-548.

Smith, M., K. Stambaugh, et al. (2009). "Surface-enhanced vibrational investigation of adsorbed analgesics." Vibrational Spectroscopy**49**(2): 288-297.

Subramani, H. J., H. K. Yeoh, et al. (2006). "Simplicity and complexity in a dripping faucet." Physics of Fluids**18**(3).

Taylor, L. S. and F. W. Langkilde (2000). "Evaluation of solid-state forms present in tablets by Raman spectroscopy." Journal of Pharmaceutical Sciences**89**(10): 1342-1353.

van Santen, E., D. M. Barends, et al. (2002). "Breaking of scored tablets: a review." European Journal of Pharmaceutics and Biopharmaceutics**53**(2): 139-145.

Vanni, M. and G. Baldi (2002). "Coagulation efficiency of colloidal particles in shear flow." Advances in Colloid and Interface Science**97**(1-3): 149-175.

Wening, K. and J. Breitkreutz (2011). "Oral drug delivery in personalized medicine: Unmet needs and novel approaches." International Journal of Pharmaceutics**404**(1-2): 1-9.